Taylor & Francis
Taylor & Francis Group

Australian Journal of Earth Sciences

An International Geoscience Journal of the Geological Society of Australia

ISSN: (Print) (Online) Journal homepage: https://www.tandfonline.com/loi/taje20

Paleosols and weathering leading up to Snowball Earth in central Australia

G. J. Retallack

To cite this article: G. J. Retallack (2021): Paleosols and weathering leading up to Snowball Earth in central Australia, Australian Journal of Earth Sciences, DOI: 10.1080/08120099.2021.1906747

To link to this article: https://doi.org/10.1080/08120099.2021.1906747

Published online: 21 May 2021.

AUSTRALIAN JOURNAL OF EARTH SCIENCES
https://doi.org/10.1080/08120099.2021.1906747

Paleosols and weathering leading up to Snowball Earth in central Australia

G. J. Retallack

Department of Earth Sciences, University of Oregon, Eugene, Oregon, USA

ABSTRACT

The Cryogenian Period (717–635 Ma), or 'Snowball Earth', was an unusually cool period of Earth history when glaciers extended to low latitudes. Past ideas on causes of this widespread glaciation include increased consumption of atmospheric carbon dioxide by silicate weathering due to continental drift into tropical paleolatitudes, or by voluminous, easily weathered volcanic tuffs. Alternatively, carbon sequestration from the atmosphere may have been intensified by advances in biomass on land or at sea. These hypotheses are tested with a new study of red siltstones of the Johnnys Creek Formation (785–717 Ma) in central Australia, where paleosols have long been recognised. Although these dolomitic red siltstones look like shales, they lack lamination. Instead, they have the massive bedding and grainsize distribution of dolomitic and calcareous loess, which precede tillites of the Areyonga Formation. Paleomagnetic studies indicate little drift from a paleolatitude of 26.2° during accumulation of the Johnnys Creek Formation. Nor does the Johnnys Creek Formation contain easily weathered volcanic ash, only local basalt flows. Paleoproductivity of the paleosols increases up section, as estimated in ppm soil CO_2 from depth in paleosols to gypsic (By) and then calcic (Bk) horizons. Deepening and intensification of soil respiration reflects greater terrestrial carbon sequestration, and increased chemical weathering up section, and both would have drawn down atmospheric CO_2. Comparable transition from gypsic to calcic soils in modern deserts reflects change from cyanobacterial-gypsic to fungal–algal calcic ecosystems. Snowball Earth glaciation may have been induced by evolutionary advances to eukaryotic and multicellular life on land, in the same way as Ordovician glaciation was induced by land plants, Permo-Carboniferous glaciation by trees, and Pleistocene glaciation by grasslands.

KEY POINTS

1. Johnnys Creek Formation of central Australia has paleosols dated 785–717 Ma.
2. Little drift from paleolatitude 26.2°, and no volcanic ash, only local basalt flows.
3. Paleosol paleoproductivity and depth of weathering increased steadily up section.
4. Glaciation may have been induced by eukaryotic and multicellular life on land.

ARTICLE HISTORY
Received 21 October 2020
Accepted 17 March 2021

KEYWORDS
Neoproterozoic; paleosol; paleokarst; Snowball Earth; central Australia

Introduction

Snowball Earth has been hypothesised as the most extensive glaciation in Earth history, extending even to tropical latitudes (Hoffman & Schrag, 2002), although a completely iced-over equator has been disputed (Moczydłowska, 2008; Retallack, 2011; Retallack *et al*., 2015). This paper examines the hypothesis that glaciation of Snowball Earth (Cryogenian 720–635 Ma) was induced by late Tonian (800–720 Ma) continental drift into carbon-sequestering, intensely weathered, warm–humid, tropical regions of small mountainous continents during the Tonian, including the Siberian, southern African and Australian cratons (Hoffman & Li, 2009; Hoffman & Schrag, 2002). Another hypothesis is increased weathering by carbonic acid of exceptionally voluminous volcanic eruption of easily weatherable materials, such as abundant volcanic tuffs in Tonian deposits of China (Long *et al*., 2019; Stern & Miller, 2018), and basalts produced by Rodinian rifting (Donnadieu *et al*., 2004), as well as degassing of sun-screening sulfate aerosols (MacDonald & Wordsworth, 2017). Another alternative is cooling by marine carbon sequestration (Tziperman *et al*., 2011), or dimethyl sulfide aerosol production (Feulner *et al*., 2015) accelerated by algal evolution in the sea. A fourth hypothesis tested here is that advances in life on land accelerated chemical weathering and carbon sequestration in soils, while fertilising the ocean with nutrient bases (Retallack *et al*., 2021). All four hypotheses for initiation of Snowball Earth invoke reduction of a CO_2 greenhouse effect, which can be quantified from paleosols (Mitchell & Sheldon, 2010; Sheldon, 2006; Sheldon & Tabor, 2013). This study gathers evidence from a sequence of paleosols before the Cryogenian, in the Johnnys Creek

CONTACT G. J. Retallack gregr@uoregon.edu Department of Geological Sciences University of Oregon 1275 East 13th Avenue, Eugene, OR 97403-1272, USA
Editorial handling: Chris Fergusson

Formation of the Bitter Springs Group in central Australia (Edgoose, 2013; Edgoose *et al*., 2018; Southgate, 1986, 1989). Petrographic and chemical data on these paleosols preceding Snowball Earth reveal not only depth and intensity of chemical weathering, but also biological paleoproductivity of soils and paleoatmospheric CO_2 levels, using previously established methods (Breecker & Retallack, 2014).

As one of the first recognised Precambrian microfossiliferous stromatolitic formations (Schopf, 1968; Walter *et al*., 1979), the Bitter Springs Group has emerged as a benchmark for the study of Proterozoic marine chemistry (Swanson-Hysell *et al*., 2012) and biology (Corkeron *et al*., 2012). However, paleosols of two kinds have long been recognised within the Bitter Springs Group: (1) red claystones with mudcracks and halite hopper casts (Schmid, 2017; Southgate, 1986, 1989), and (2) rubbly dolostone filling paleokarst relief (Lindsay, 1987, 1989; Skotnicki *et al*., 2008). Both kinds of paleosols have been controversial in Ediacaran rocks (Gehling & Droser, 2013; Retallack, 2013a, 2016), and subsequent studies of the Johnnys Creek Formation (Swanson-Hysell *et al*., 2012) have assumed that it was entirely marine and a record of global ocean change. Were nodular, red beds, paleosols (Retallack, 2013a), or shallow marine sandstones (Gehling & Droser, 2013)? Was the basal Ediacaran, Nuccaleena Formation, 'cap carbonate' a calcareous loess (Retallack, 2011), or an exceptional global oceanic alkalinisation (Yu *et al*., 2020)? Were the Wonoka Canyons valley paleokarst (Retallack *et al*., 2014), or submarine canyons (Giddings *et al*., 2010)? These alternatives have consequences for interpreting whether associated isotopic anomalies (Kennedy, 2013; Knauth & Kennedy, 2009; Morteani *et al*., 2007), and fossils (Retallack, 2013a, 2016) represent early life on land or at sea. Terrestrial diagenetic and marine interpretations of 'cap carbonates' are relevant also for understanding the Johnnys Creek Formation, which has petrographic textures and isotopic anomalies comparable with 'cap carbonates'. Each of the four hypotheses for the causes of Snowball Earth by weathering changes due to continental drift (Hoffman & Schrag, 2002), volcanic eruption (Long *et al*., 2019), marine fertilisation (Tziperman *et al*., 2011), or terrestrial productivity (Retallack *et al*., 2021) is assessed here from the new perspective of paleosols in the Johnnys Creek Formation.

Geological background

The Bitter Springs Group of central Australia (Figures 1 and 2) is famous for its stromatolites (Corkeron *et al*., 2012; Grey *et al*., 2012; Southgate, 1989; Walter *et al*., 1979), permineralised microfossils (House *et al*., 2000; Oehler, 1976, 1977; Schopf, 1968; Schopf & Blacic, 1971) and acritarchs (Zang & Walter, 1992), but also has non-marine evaporitic

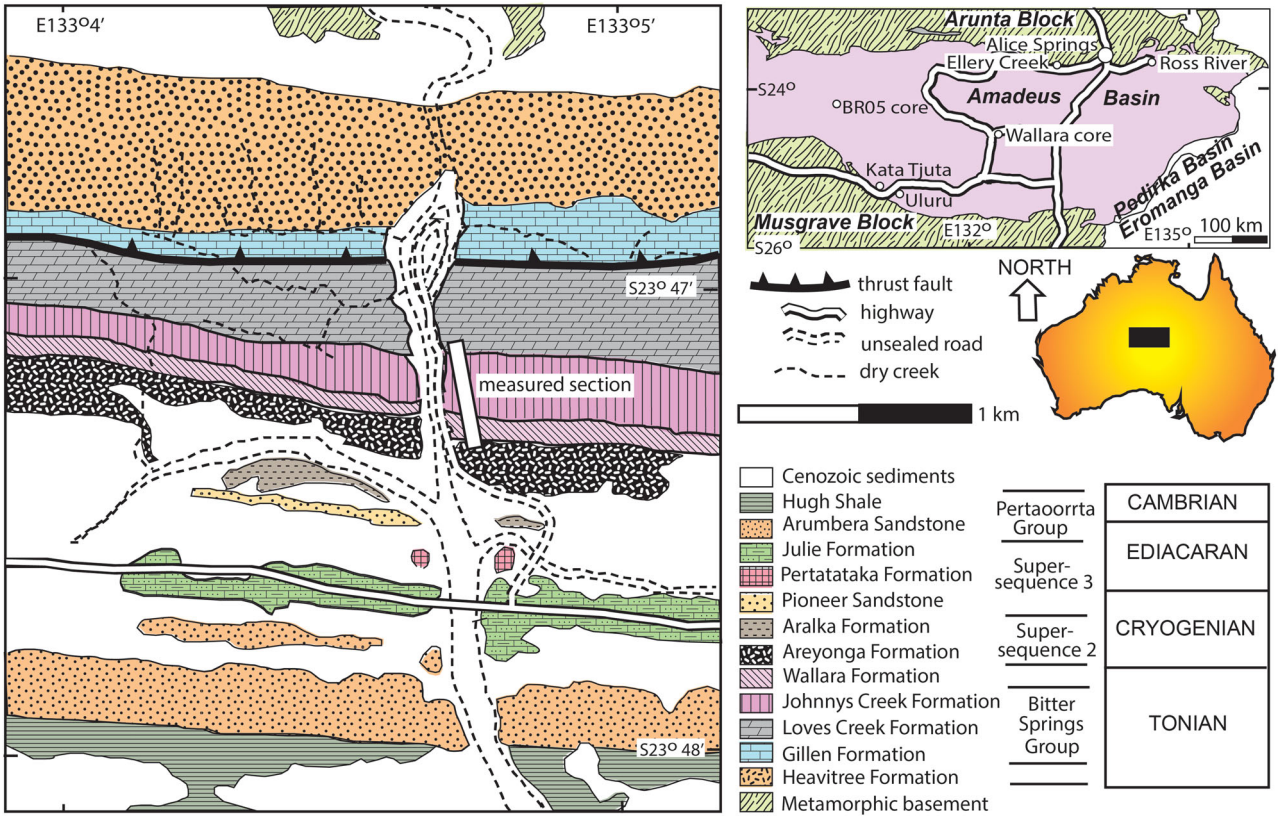

Figure 1. Sample and study locations for evidence of changes in chemical weathering during deposition of the Johnnys Creek and Wallara formations in central Australia. Geological map modified from Edgoose (2013), following Klaebe *et al*. (2017) and Swanson-Hysell *et al*. (2012). Supersequences of Walter *et al*. (1995) include Supersequence 1 (Heavitree to Wallara formations) and Supersequence 4 (above Julie Formation).

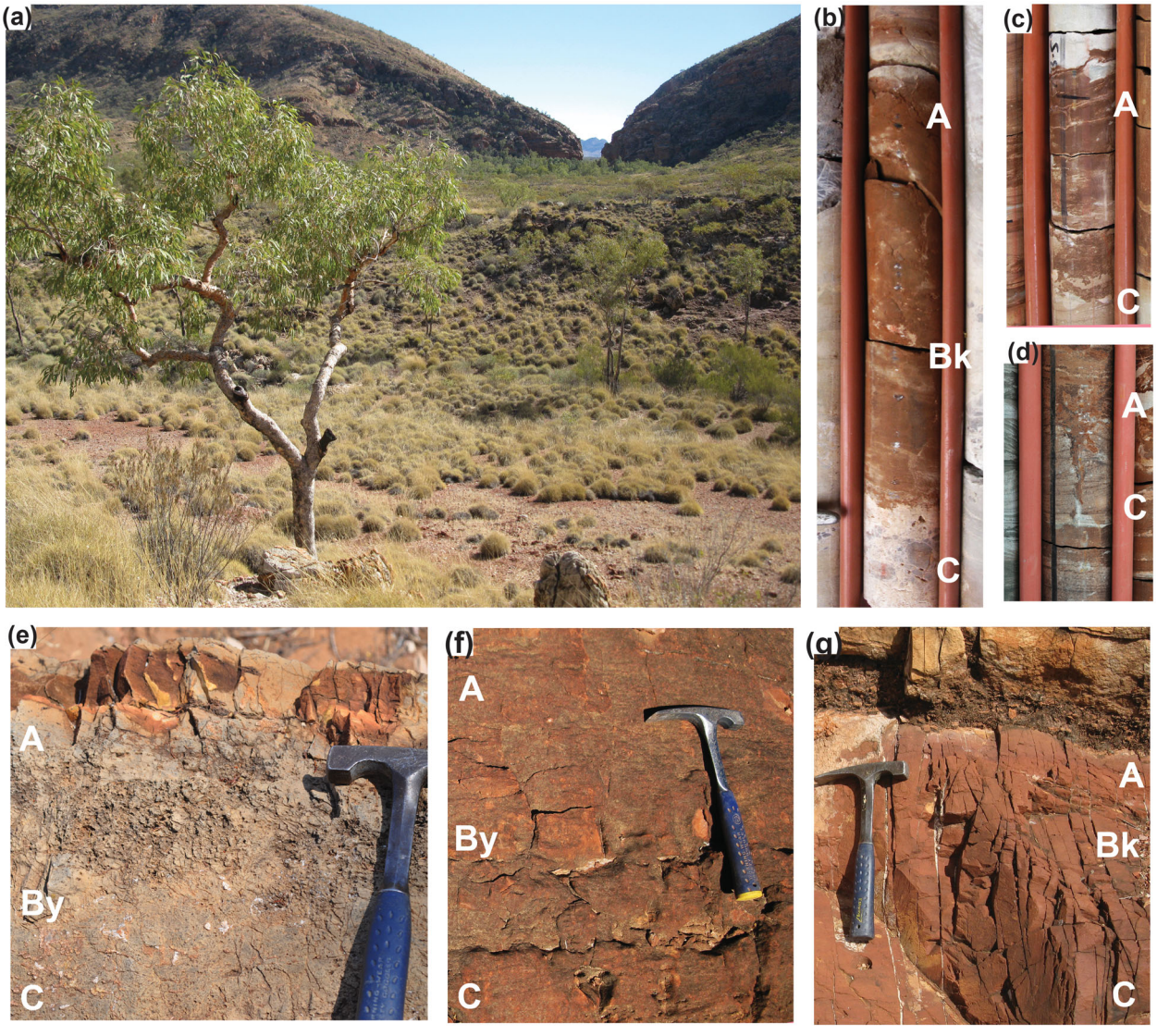

Figure 2. Field photographs of measured section of Ellery Creek, Northern Territory (a, e–g) and in core BR05 (b–d): (a) overview of recessive weathering paleosols of the Johnnys Creek Formation and plateau of stromatolitic limestone of the Loves Creek Formation toward gap in ridge of Heavitree Formation at Ellery Big Hole; (b) Akngerre (Calcid) paleosol (607.7 m in Figure 4); (c) Kwerralye paleosol (Ochrept) paleosol (704.1 m in Figure 4); (d) Itwe (Fluvent) paleosol (856.7 m in Figure 4); (e) Alkynge (Gypsid) paleosol in upper Loves Creek Formation (350 m in Figure 3); (f) Alkynge (Gypsid) paleosol in Johnnys Creek Formation (390 m in Figure 3); (g) Akngerre (Calcid) paleosol in Johnnys Creek Formation (503 m in Figure 3). Bold white codes are interpreted ancient soil horizons, including surface horizon (A), gypsic horizon (By), calcic horizon (Bk), and parent material (C).

red siltstones (Hill *et al.*, 2000; Southgate, 1986, 1989). The Gillen, Loves Creek and Johnnys Creek formations were once members of the Bitter Springs Formation (Southgate, 1986; Swanson-Hysell et al., 2012; Walter *et al.*, 1995), but were elevated to formations of the Bitter Springs Group (Edgoose *et al.*, 2018; Normington, Beyer, *et al.*, 2019). The upper part of the Johnnys Creek Formation had been assigned to 'Finke beds' (Grey *et al.*, 2012), but that name was already occupied (Haines & Allen, 2014), and the uppermost portion of what used to be called Johnnys Creek Formation is now known as Wallara Formation (Normington, Edgoose, *et al.*, 2019).

From Australia-wide stromatolite biostratigraphy, the Tonian *Acaciella australica* assemblage of the Loves Creek and Johnnys Creek formations (Walter, 1972, 1976) is distinct from the early Tonian *Tungussia erecta* assemblage of the Gillen Formation (Grey & Corkeron, 1998), and the late Tonian *Baicalia burra* assemblage of the overlying Wallara Formation (Grey *et al.*, 2012). Both predate the *Elleria minuta* Assemblage of the Cryogenian Pioneer Sandstone and the *Tungussia julia* assemblage of the Ediacaran Julie Formation in Ellery Creek (Walter *et al.*, 1979).

Maximum depositional age of detrital zircons of the Johnnys Creek Formation by SHRIMP U–Pb is 1029 ± 23 Ma, and for the Wallara Formation is 1006 ± 13 Ma (Kositcin *et al.*, 2015; Normington, Beyer, *et al.*, 2019). Continental tholeiitic basalts (Barovich & Foden, 2000) in the lower Johnnys Creek Formation in the northeastern part of the

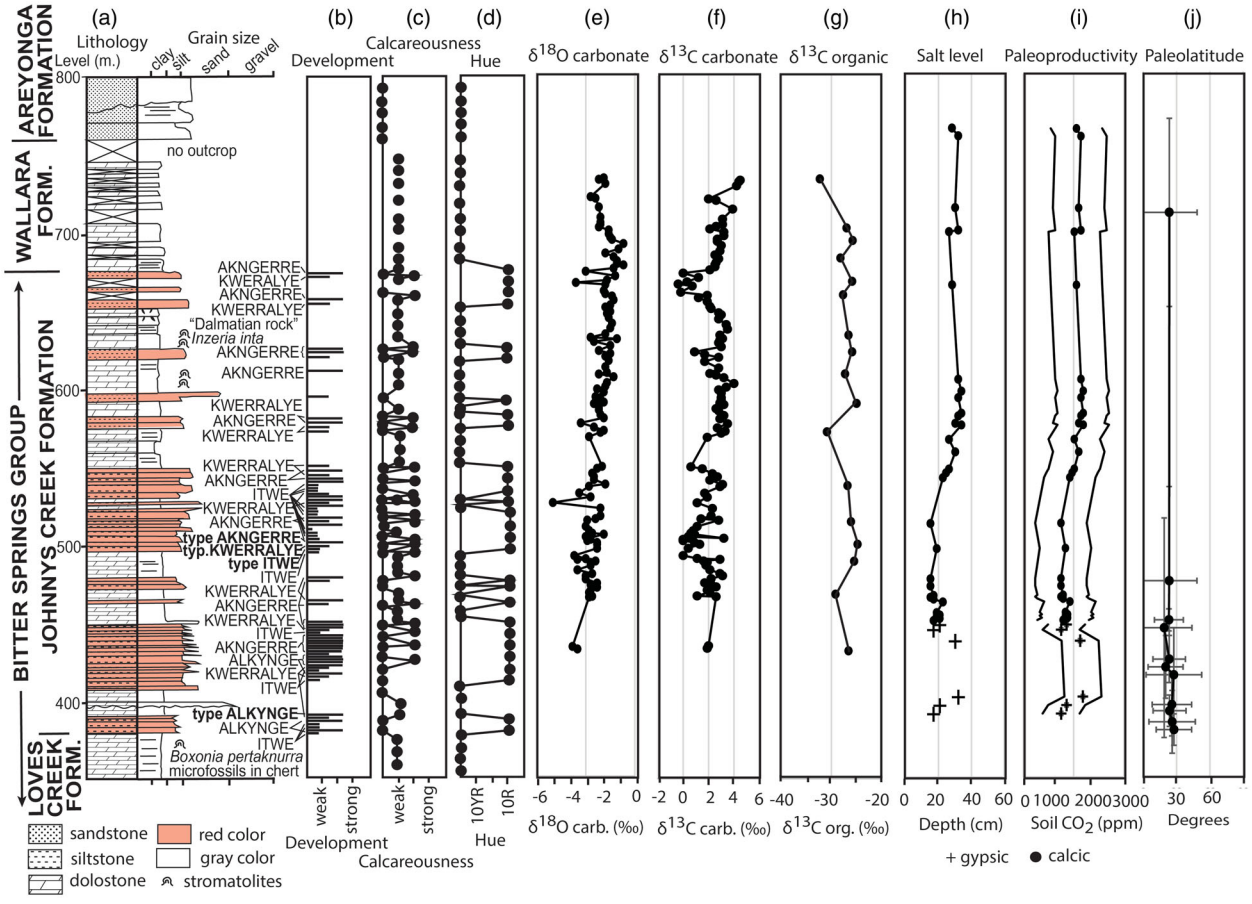

Figure 3. Geological section and a variety of proxy measures of the Johnnys Creek Formation in Ellery Creek (starting at S23.78387°E133.07433°): (a) lithological log; (b) paleosol position and degree of development (scale of Retallack, 2019); (c) reaction with dilute HCl (scale of Retallack, 2019); (d) Munsell hue; (e–g) stable isotopic data from Swanson-Hysell *et al*., 2012); (h) depth within paleosols to carbonate nodules and gypsum crystals; (i) inferred soil paleoproductivity (from method of Breecker & Retallack, 2014); and (j) paleolatitude (from Swanson-Hysell *et al*., 2012).

Amadeus Basin have been correlated using REE and εNd with the Amata Dolerite of the Musgrave Block to the south, where it has been dated by Sm–Nd at 790 ± 40 and 797 ± 49 Ma (Zhao *et al*., 1994). Other Sm–Nd ages for comparable dolerites of the Musgrave Block are 747 ± 48 and 766 ± 53 Ma (Werner *et al*., 2018). Better tie points for an age model for the Johnnys Creek Formation may be inflections in the carbon isotopic composition of carbonate (Figures 3 and 4). These isotopic inflexions are not dramatic changes in isotopic composition of the world ocean, because high isotopic values are from marine, stromatolitic limestones, but low values are from non-marine, red, dolomitic siltstones (Klaebe *et al*., 2017). Isotopic infections are thus marine–non-marine oscillation and reflect changes in global sea-level correlative with other regions with better radiometric dates (MacDonald *et al*., 2010; MacLennan *et al*., 2020). These dated isotopic inflections used for correlation by Swanson-Hysell *et al*. (2010, 2012) are as follows: (1) 811.5 Ma swing to positive values at base of Bitter Springs Anomaly (MacDonald *et al*., 2010) at 1224.8 m in BRO5 core and 170 m in Ellery Creek; (2) 785 Ma swing to negative values at top of Bitter Springs Anomaly (Swanson-Hysell *et al*., 2012) at 1089 m in BR05 core and 380 m in Ellery Creek; (3) 752.1 Ma negative spike of Konnarock Glaciation (MacLennan *et al*., 2020) at 684.6 m in BR05 core and 591 m in Ellery Creek; and (4) 717.4 Ma isotopic decline below tillite (Swanson-Hyssell *et al*., 2012) at 532m in BR05 core and 767 m in Ellery Creek. This gives a duration of 785–717 Ma for the Johnnys Creek Formation using equations of Table 1.

Past interpretations of sedimentary environments and facies of the Johnnys Creek Formation are summarised in Table 2. Paleokarst breccias are common in the upper part of both the Loves Creek and Johnnys Creek formations, representing intervals of subaerial exposure and erosion of a sequence of subtidal to supratidal stromatolitic dolostones and interbedded sabkha and coastal plain deposits (Klaebe *et al*., 2017; Skotnicki *et al*., 2008; Southgate, 1986, 1989, 1991).

Materials and methods

Red siltstones of the Johnnys Creek Formation are poorly exposed in outcrop along Ellery Creek (Figures 1 and 2a, f, g; Edgoose, 2013), but were also inspected in drill core of Bloods Range 5 (BR05DDH01: Ambrose *et al*., 2010; Normington, Beyer, et al., 2019; Smith, 2011) housed in the

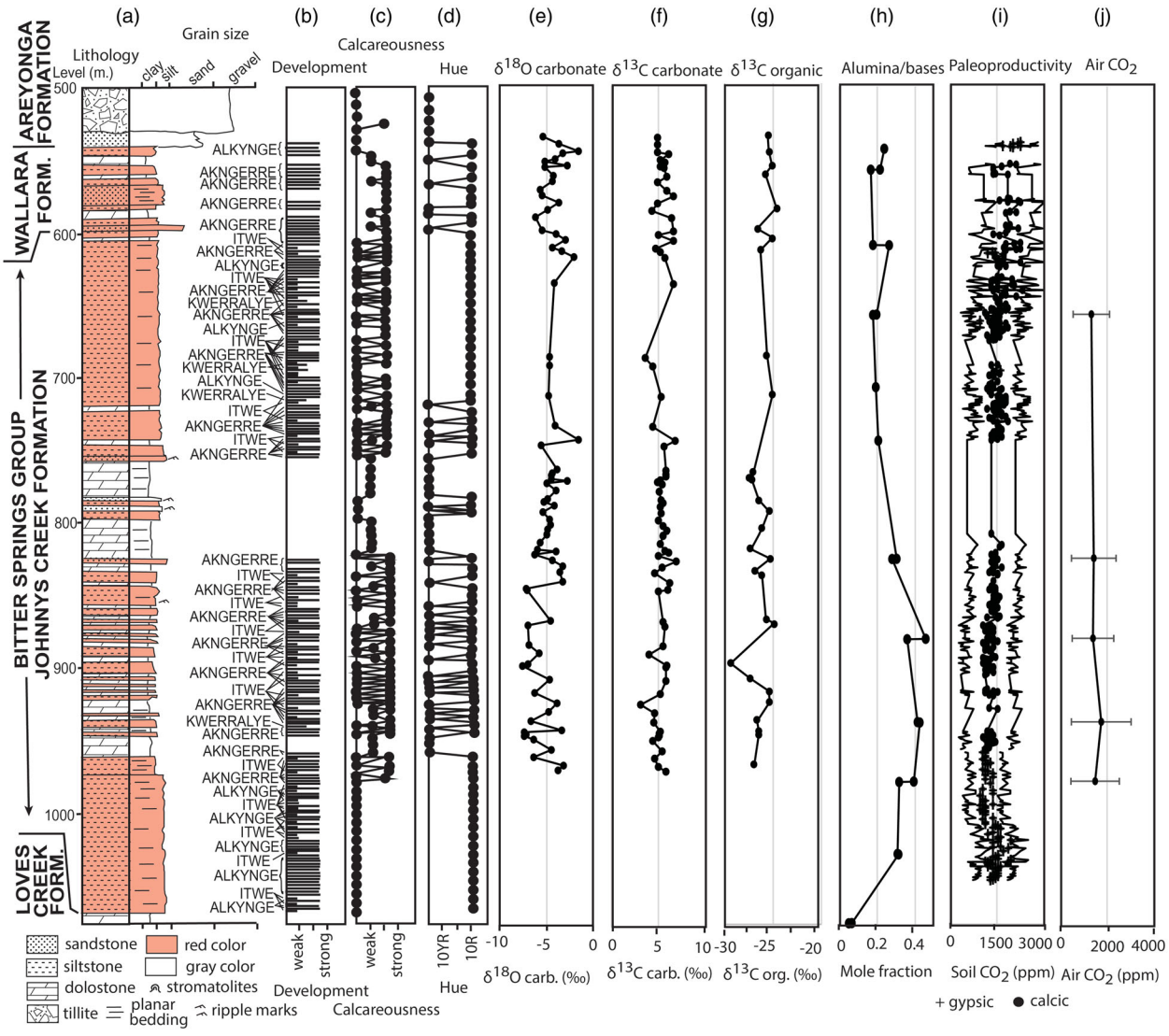

Figure 4. Geological section and a variety of proxy measures of the Johnnys Creek Formation in Bloods Range 05 (BR05) core (S24.4556878°E130.382509°): (a) lithological log; (b) paleosol position and degree of development (scale of Retallack, 2019); (c) reaction with dilute HCl (scale of Retallack, 2019); (d) Munsell hue; (e–g) stable isotopic data from Swanson-Hysell *et al*., 2012); (h) alumna/bases molar ratio as a weathering index (from Table S2); (i) inferred soil paleoproductivity (from method of Breeker & Retallack *et al*., 2014); and (j) atmospheric CO_2 (from method of Breecker & Retallack, 2014).

Northern Territory Geological Survey Core Facility in Alice Springs (Figure 2d). Detailed stratigraphic sections were measured in Ellery Creek (Figure 3) and the BR05DDH01 core (Figure 4), and oriented rock samples were collected of suspected paleosols for laboratory studies, including bulk chemical composition (Online data, Supplementary Table S1). Thin-sections were used to quantify grainsize (Supplementary Table S2) and mineral compositions (Supplementary Table S3) by point counting (500 points) using a Swift automated stage and Hacker counting box on a Leitz Orthoplan Pol research microscope. This same apparatus was also used to determine grainsize distributions by measuring the long axis of 1000 grains using a calibrated ocular micrometre. Accuracy of such point counts is ±2% for common constituents (Murphy, 1983). These rocks are too firmly cemented, compacted and clay-poor for fractionation-settling determination of grainsize. Major- and trace-element chemical analysis was determined by XRF in fused beads at ALS Chemex in Vancouver, Canada. Bulk density was measured by the clod method: from raw weight, then clods coated in paraffin of known density, in and out of chilled water (Blake & Hartge, 1986). Stable isotope values ($\delta^{18}O$ and $\delta^{13}C$) of 50 mg samples of carbonate nodules were determined using a10-kV Finnigan MAT 253 mass spectrometer in the University of Oregon laboratory of Ilya Bindeman (Table 3), with error of both $\delta^{18}O$ and $\delta^{13}C$ of ± 0.03‰. These data supplement large datasets of comparable isotopic data for dolomitic siltstone and dolostone of the Johnnys Creek Formation published by Swanson-Hysell *et al*. (2010).

Table 1. Equations for geological age and paleoenvironmental reconstructions of paleosols.

Equation	Input variables	R^2	SD	P	Reference
$y = 0.124x + 657.64$	Age (y, Ma) in Ellery Creek, height (x, m) in stratigraphic section	0.98	±48	0.002	Herein
$\mathbf{y} = -0.5183\mathbf{x} + 841.74$	Age (y, Ma) in core BR05, depth (x, m) in core	0.97	±34	0.006	Herein
$\mathbf{C} = \frac{-0.51 \times 100}{\left\{\left(\frac{\frac{0.49}{\mathbf{B}}}{\mathbf{e}^{0.27}}\right) - 1\right\}}$	Compaction (C, fraction) due to depth of burial (B, km) by overburden	0	0	0	Sheldon and Retallack (2001)
$\varepsilon_{\mathbf{i,w}} = \left[\frac{\rho_{\mathbf{p}} \mathbf{C}_{\mathbf{j,p}}}{\rho_{\mathbf{w}} \mathbf{C}_{\mathbf{j,w}}}\right] - 1$	Strain (ε) due to soil formation (mole fraction), immobile element (i = Ti, wt%), bulk density (ρ, g.cm^{-3}), oxide assay (C, wt%), for elements (subscript i,j) of weathered material (subscript w) and parent material (subscript p)	0	0	0	Brimhall *et al.* (1992)
$\tau_{\mathbf{j,w}} = \left[\frac{\rho_{\mathbf{w}} \mathbf{C}_{\mathbf{j,w}}}{\rho_{\mathbf{p}} \mathbf{C}_{\mathbf{j,p}}}\right][\varepsilon_{\mathbf{i,w}} + 1] - 1$	Mass transfer (τ, mole fraction) due to soil formation, rest as above	0	0	0	Brimhall *et al.* (1992)
$\boldsymbol{A} = 3.92\boldsymbol{D}^{0.34}$	Age (A, kyrs) of paleosol, diameter (D, cm) of pedogenic carbonate nodules	0.57	±1.8	0.001	Retallack (2005)
$\boldsymbol{A} = 3.987\boldsymbol{G} + 5.774$	Age (A, kyrs) of paleosol, abundance of gypsum (G, % surface area)	0.95	±15	0.01	Retallack, Dunn, *et al.* (2013)
$\boldsymbol{P} = 137.24 + 6.45\boldsymbol{D} - 0.0132\boldsymbol{D}^2$	Mean annual precipitation (P, mm), depth in profile to calcareous nodules (D, cm), corrected for burial compaction	0.52	±147	0.0001	Retallack (2005)
$\boldsymbol{P} = 87.593\boldsymbol{e}^{0.0209\boldsymbol{D}}$	Mean annual precipitation (P, mm), depth to gypsum (D, cm) corrected for burial compaction	0.63	±129	0.0001	Retallack and Huang (2010)
$\boldsymbol{R} = 0.79\,\boldsymbol{T} + 13.7$	Seasonality or wettest minus driest month precipitation (R, mm), thickness of the calcic horizon (T, cm)	0.58	±22	0.0001	Retallack (2005)
$\boldsymbol{T} = -18.5\,\mathbf{M} + 17.3$	Mean annual temperature (T, °C), ratio of soda + potash/alumina (M, mole fraction)	0.37	±4.4	0.0001	Retallack (2005)
$\boldsymbol{P_a} = \boldsymbol{P_r} \cdot \frac{\left(\delta^{13}\mathbf{C_s} - 1.0044\delta^{13}\mathbf{C_r} - 4.4\right)}{\left(\delta^{13}\mathbf{C_a} - \delta^{13}\mathbf{C_s}\right)}$	Atmospheric CO_2 (P_a, ppmv), soil-respired CO_2 (P_r, ppmv), carbon isotopic composition of soil CO_2 ($\delta^{13}C_s$, ‰), carbon isotopic composition of soil-respired CO_2 ($\delta^{13}C_s$, ‰), carbon isotopic composition of air ($\delta^{13}C_a$, ‰)	0	0	0	Cerling (1991)
$\boldsymbol{\delta}^{13}\mathbf{C_s} = \frac{\left(\delta^{13}\mathbf{C_c} + 1000\right)}{\frac{(11.98 - 0.12\mathbf{T})}{1000}} - 1000$	Carbon isotopic composition of soil CO_2 ($\delta^{13}C_s$, ‰), carbon isotopic composition of pedogenic carbonate ($\delta^{13}C_c$, ‰), temperature at time of carbonate precipitation (T, °C)	0.93	±0.28	0.0001	Romanek *et al.* (1992)
$\boldsymbol{\delta}^{13}\mathbf{C_a} = 0.665\boldsymbol{\delta}^{13}\mathbf{C_o} + 6.128$	Carbon isotopic composition of CO_2 in air ($\delta^{13}C_a$, ‰), carbon isotopic composition of soil organic matter ($\delta^{13}C_o$, ‰)	0.96	±1.73	0.0001	Fletcher *et al.* (2005)
$\boldsymbol{P_r} = 25.3\boldsymbol{D_c} + 588$	Soil-respired CO_2 (P_r, ppmv), original depth to pedogenic carbonate corrected for burial compaction (D_c, cm)	0.66	±768	0.0001	Breecker and Retallack (2014)
$\boldsymbol{P_r} = 42.9\boldsymbol{D_g} + 399$	Soil-respired CO_2 (P_r, ppmv), original depth to pedogenic gypsum corrected for burial compaction (D_g, cm)	0.64	±552	0.05	Breecker and Retallack (2014)

Table 2. Sedimentary facies of the Johnnys Creek Formation.

Facies	Interpretation	Author
Stromatolitic dolostone	Lacustrine, lagoonal or intertidal stromatolite reefs	Klaebe *et al.*, 2017; Schmid, 2017; Southgate, 1986, 1989
Dalmatian rock dolostone	Gas escape structures in dolomitic mud	Edgoose, 2013
Dolomite grainstone	Beach and shoreface peloids, ooids and intraclasts	Klaebe *et al.*, 2017; Southgate, 1986, 1989
Dolomite breccia	Paleokarst cave fill	Klaebe *et al.*, 2017; Skotnicki *et al.*, 2008
Red dolo-mudstone	Gypsiferous soils of playa lake or sabkha	Klaebe *et al.*, 2017; Schmid, 2017; Southgate, 1986, 1989

Table 3. New carbonate stable isotopic analyses and atmospheric CO_2 estimates from Johnnys Creek Formation in BR05DDH01 core.

Specimen	Depth (m)	$\delta^{13}C_{carb}$ (‰ VPDB)	$\delta^{18}O_{carb}$ (‰ VPDB)	$\delta^{13}C_{org}$ (‰ VPDB)	Paleotemperature (°C)	Depth to Bk (cm)	Soil CO_2 (ppm)	Atmospheric CO_2 (ppm)
R4240	655.0	−2.80	−8.10	−25.7	6.8	15	1339	1321 ± 787
R4246	820.7	−1.79	−4.00	−25.3	7.9	11	1141	1428 ± 961
R4248	875.2	−1.47	−5.23	−24.9	6.3	12	1192	1393 ± 898
R4250	932.0	−1.92	−4.84	−26.7	6.8	9	1041	1750 ± 1291
R4252	972.4	−2.90	−6.88	−27.0	6.1	10	1092	1485 ± 1044

All analyses are calcite nodules from Akngerre paleosols in core BR05DDH1 analysed at University of Oregon. The specimens are in the collection of Museum of Natural and Cultural History, University of Oregon, and depth is below the surface in the borehole. Organic isotopic values are from Swanson-Hysell *et al.* (2010). Paleotemperature calculated and observed depth to Bk can be corrected for burial compaction using equations in Table 1.

Metamorphic and diagenetic alteration

Paleosols are a form of early diagenesis, which must be distinguished from late diagenesis and metamorphism before paleoenvironmental interpretation. The Johnnys Creek Formation demonstrates three early diagenetic alterations common in red beds: (1) drab mottles in upper portions of beds due to burial gleisation of buried organic matter, (2) dark red (Munsell 10 R) colour from dehydration reddening of ferric hydroxide minerals, and (3) substantial lithostatic compaction (Retallack, 1991a). Burial gleisation is chemical reduction of oxides and hydroxides of iron by anaerobic bacteria on subsidence into anoxic water and is especially suggested by drab mottles and tubular features radiating down from bed tops (Figure 2b, g), as in Cambrian (Álvaro *et al*., 2003; Retallack, 2008) and Proterozoic red beds (Driese *et al*., 1995; Retallack, 2013a). Such geologically ancient red beds are also purple to red in colour from burial dehydration of ferric oxyhydroxides (Figure 2b–d, f, g), unlike brown to yellow modern soils and late Pleistocene sediments (Retallack, 1991a).

Complex folding and thrusting of the Amadeus Basin during the mid-Paleozoic (450–300 Ma) Alice Springs Orogeny, tilted the Johnnys Creek Formation to 43°N on strike 68° without obvious faults or folds, like those apparent lower in the Ellery Creek section (Figure 1). With highly variable K_2O values of 1.82–6.67 wt % (Table S1), there is little evidence of pervasive potash metasomatism (Novoselov & de Souza Filho, 2015). The Johnnys Creek Formation was deeply buried by 6.3 km of overburden (Edgoose, 2013; Grey *et al*., 2012). Burial compaction (*C* as wt%) expected for 6.3 km burial can be calculated as 53%. These calculations use a formula in Table 1 with depth of burial (*B* in km) and 0.51, 0.49 and 0.27 as physical constants (of Sheldon & Retallack, 2001). Compaction estimates are needed for paleoenvironmental interpretations from bed thicknesses (Retallack, 2005).

Paleosol recognition

Paleosols are definitively recognised in the field as horizons of fossil root traces (Retallack, 1977, 1991b), but in rocks too old for vascular land plants (Retallack, 2015a) a variety of other features can be used to recognise paleosols. These include field recognition of soil cracking structures and pseudomorphs of soluble salts (Southgate, 1986, 1989). The following paragraphs consider each of these paleosol criteria in turn.

Angular silt grains

Thin-section examination of what appear to be red mudstones of the Johnnys Creek Formation are really siltstones with abundant, angular, silt-size grains (Figure 5). Measurement of the long axis of 1000 grains in two specimens (R5394 and R5396) showed means of 5.4 ± 1.0 and 5.0 ± 1.1 Φ (0.03 ± 0.04 and 0.05 ± 0.06 mm), respectively (Figure 6a), which is moderately well-sorted silt. These rocks are not the claystones they appear to be in hand specimen, but are mostly grain-supported angular silt grains, with scattered clasts of sand size. Point counting showed that these two specimens had 61.4 and 71.2 vol% silt grains (Table S2), and 11.8 and 51.4 vol% dolomite clasts, respectively (Figure 5; Table S3). These red siltstones are distinct from sand to granule size of neomorphically recrystallised grey dolostones with stromatolites in the same section, and also contain mud cracks, halite hopper casts, and gypsum crystals (Klaebe *et al*., 2017; Southgate, 1986, 1989).

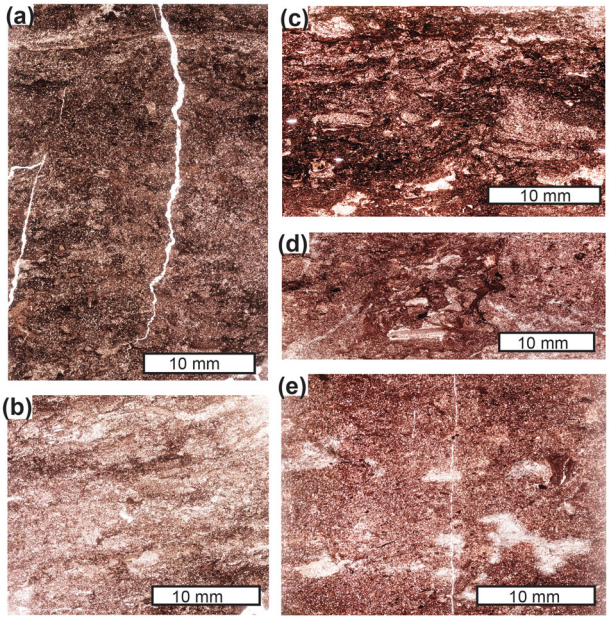

Figure 5. Petrography of Akgnerre (a, b) and Alkygnge (c–e) paleosols in pre-Cryogenian (800–720 Ma) Johnnys Creek Formation in Ellery Creek, all thin-sections oriented up to top and perpendicular to bedding: (a) sharp top to A horizon R5168; (b) micritic nodules of Bk horizon R5170; (c) brecciated above A horizon R5176; (d) breccia fill to deep crack R5177: and (e) gypsum crystals of By horizon R5178.

Vertically oriented thin-sections of the Johnnys Creek Formation are massive (Figure 5), and lack lamination or varves found in marine or lacustrine shales. While much eolian silt may have fallen into the sea before landscapes were stabilised by plants, silt grains are supported by clay and carbonate in Cambrian marine rocks (Dalrymple *et al*., 1985), rather than grain-supported as in the Johnnys Creek Formation (Figure 5a). Grainsize distribution and mineral composition of Johnnys Creek Formation red siltstones are here interpreted as Tonian loess, because they are similar in grainsize and texture to Quaternary Peoria Loess (Pye & Sherwin, 1999). Peoria Loess of Kansas and Nebraska is weakly calcareous and volcaniclastic (Swineford & Frye, 1951), but strongly calcareous in Illinois, Indiana, and Mississippi (Bettis *et al*., 2003). Peoria Loess is 42% carbonate at Vicksburg, Mississippi (Fisk, 1951), 32% at Cumback, Indiana (Ruhe & Olson, 1980) and 31% in core G56 in Illinois 80 km north of St. Louis (Grimley *et al*., 1998). These

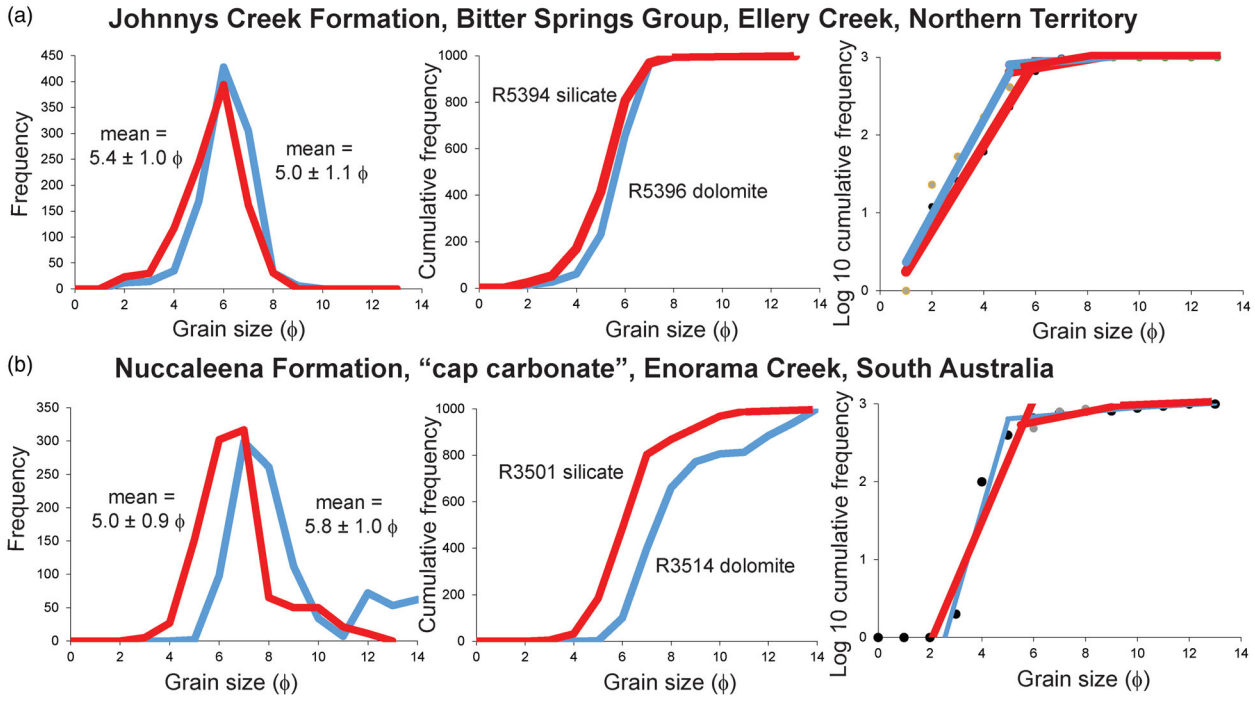

Figure 6. Grainsize distribution of red siltstones of the Tonian Johnnys Creek Formation (a) compared with comparable calcareous siltstones (b) of a 'cap carbonate', the basal Ediacaran Nuccaleena Formation of South Australia (from Retallack, 2011).

compositional differences reflect proximity to Cordilleran volcanoes in Kansas and Nebraska, but proximity to freshly deglaciated Paleozoic limestones and dolostones from Illinois to Mississippi. Another similar eolian deposit is the basal Ediacaran Nuccaleena Formation of South Australia, which also is rich in dolomite, quartz, and feldspar like the Johnnys Creek Formation (Retallack, 2011). Red calcareous paleosols and a suite of eolian structures, including climbing translatent stratification, are evidence against prior interpretations of the Nuccaleena Formation as a marine dolostone (Yu *et al*., 2020).

Crack patterns

Desiccation crack polygons from the Love Creek and Johnnys Creek formations are illustrated by Klaebe *et al*. (2017) and Southgate (1989). Cracks with the v-shaped profile of desiccation cracks (Weinberger, 2001) were seen at several levels in the Johnnys Creek Formation, including examples extending down into sandstone (Figure 2c). These sandstone cracks emanate from the most hematite-rich tops of sandy beds, and the enigma of sand cracking like clay as explained by Prave (2002) is due to abundant hydrated microbiota, like that of a microbial earth soil (Retallack, 2012). An alternative explanation may be frost cracking in a periglacial soil (Kokelj *et al*., 2007; Raffi & Stenni, 2011); however, ice wedges are characteristically more strongly tapering than this example (Figure 2c).

Soils have more complex cracks than simple desiccation polygons, revealed by surface modifications known as cutans (Retallack, 2019). Thin, near-vertical cracks, stained with iron and aluminium (thus sesquans in soil cutan terminology) have been folded by compaction below the laminated cover to paleosols, and are especially obvious in vertically oriented thin-sections of the Johnnys Creek Formation (Figure 5a, c). A complex systems of cracks in the Johnnys Creek Formation destroyed original lamination except in the deepest parts of beds where they overlie the cracked surface of the underlying bed. These cracks define characteristic units of soil structure known as blocky angular peds (Retallack, 2019). Marine or lacustrine shales, in contrast, have uncracked, clear, lamination, or varves (Retallack & Jahren, 2008; Zillen *et al*., 2008), not seen in the Johnnys Creek Formation.

Gypsum sand crystals

The Loves Creek and Johnnys Creek formations preserve evidence of a variety of evaporite minerals: halite hopper casts, gypsum sand crystals, and clear anhydrite (Klaebe *et al*., 2017; Schmid, 2017; Southgate, 1989). Original halite has not been recorded, but the upper Loves Creek Formation has cubic to triangular casts in siltstone with hopper-like pyramidal hollows on cube faces and internal zoning of bowed-in faces. Limpid tabular crystals of gypsum and anhydrite are rare in red siltstones of the Johnnys Creek Formation (Figure 2e, f). There are also small radiating crystal clusters of unferruginised, poikilotopic, crystals (Figure 5e), commonly called 'sand crystals' or 'desert roses' (Retallack, 2019).

These different forms represent a spectrum of conditions from marine precipitation to formation in soils.

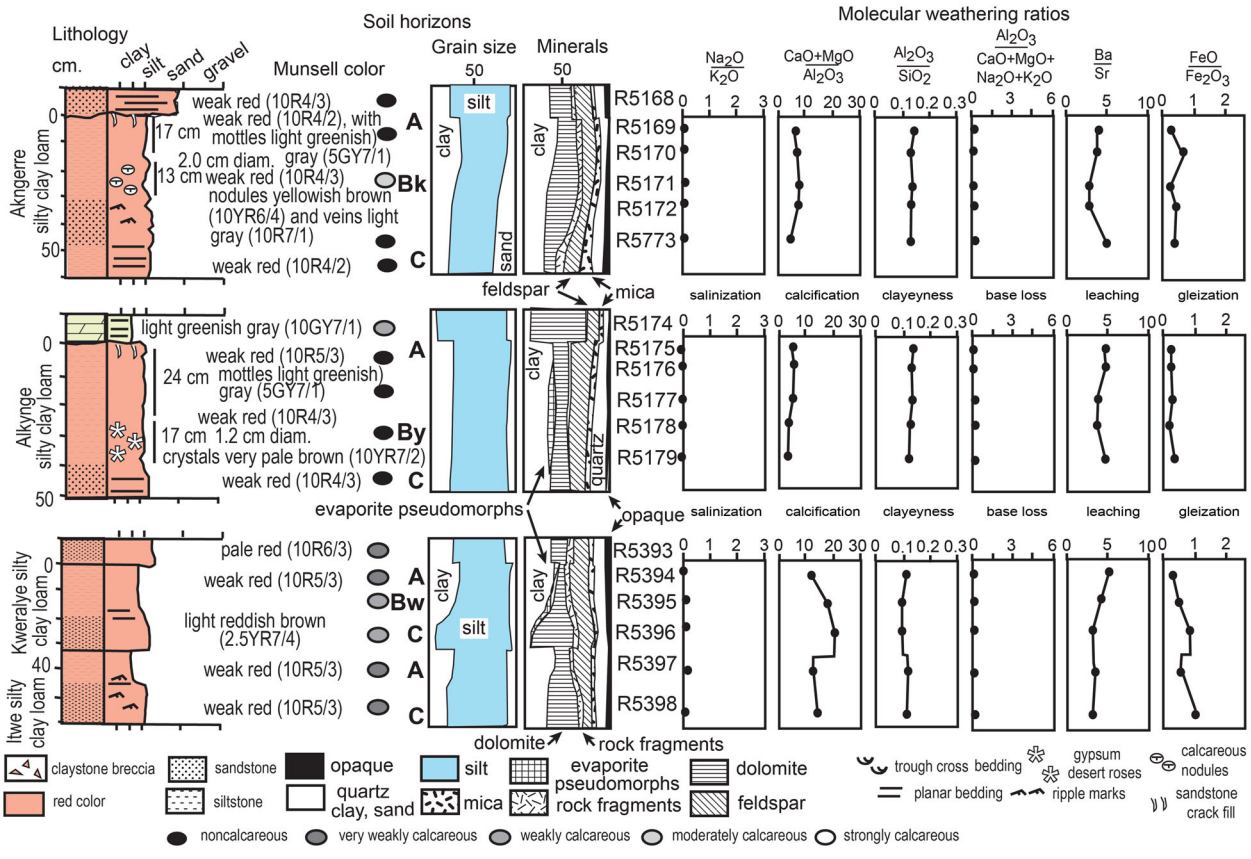

Figure 7. Paleosol profiles from the Johnnys Creek Formation, their petrographic composition from point counting thin-sections, and weathering trends revealed by molecular weathering ratios (Tables 2–4). Stratigraphic levels of these profiles are labelled in boldface in Figure 3.

Limpid crystals and seams of gypsum and anhydrite form in marginal marine or lacustrine sabkhas, where clear crystals precipitate from solution to displace surrounding grains of saturated sediment (Renaut & Tiecerlin, 1994; Ziegenbalg *et al*., 2010). Hopper casts of halite with bowed zoning reveal sequential precipitation from solution, and then dissolution in rain or subsequent inundation, and covering (Eriksson *et al*., 2005). Gypsum sand crystals on the other hand form by replacement and cementation without extensive displacement of matrix within the confining pressure of desert soil and dried-out playa lake beds and are commonly known as desert roses (Al-Kofahi *et al*., 1993; Watson, 1985). As in gypsic horizons of desert soils (Retallack & Huang, 2010), sand crystals are organised into subsurface (By) horizons (Figures 2e, f and 7).

Calcareous nodular horizons

Testing in the field with dilute HCl at Ellery Creek and in the BR05 core yielded effervescence on only a few nodular horizons. Red siltstones of the Johnnys Creek Formation are largely non-effervescent dolomitic silt (Figure 7), amenable to stable isotopic analysis (Figures 3e, f and 4e, f). The few effervescent patches proved to be low-magnesium calcite nodules (Figure 2g), generally in the size range 3–4 mm, but in places coalescing into larger masses. Their micritic cement is replacive rather than displacive (Figure 5b).

Low-magnesium calcite nodules are also aggregated into subsurface horizons (Figure 7), and their replacive, micritic microtexture with circumgranular cracks is evidence that they were calcic (Bk) horizons of soils (Retallack, 2005). Marine or lacustrine stromatolitic carbonates of the Loves Creek and Johnnys Creek formations on the other hand are very different: dolomitic, grey in colour, well laminated, and with very uneven grainsize including large crystals due to burial neomorphism (Klaebe *et al*., 2017; Southgate, 1989). Especially striking are wide (5–7 mm), black, sparry calcite, tubes within light grey saccharoidal dolomite at one level of the Johnnys Creek Formation in Ellery Creek called 'Dalmatian rock' (656 m in Figure 3). 'Dalmatian rock' has been attributed to soft-sediment deformation of limestone nodules in dolomicrite (Edgoose, 2013). This distinctive banded limestone may be the source of microfossils in calcite illustrated by Folk and Chafetz (2000).

Mineral abundance trends within beds

Point counting of individual beds shows abundant dolomite grains throughout each bed, but little depletion of rock fragments and feldspar near the surface (Figure 7). Clay enrichment toward the surface of beds is abruptly

truncated below sharp grainsize discontinuities with overlying siltstone and sandstone, and clay is confined to intervals only 5–15 cm thick. Dolomite is depleted near the top of the profiles but is very abundant at the base of beds. The dolomite rhombs are rounded, have darkened edges, and are separated by intervening red clay. Dolomite grains in red siltstones are not interlocking and clean of clay like dolomite in stromatolitic units within the Johnnys Creek Formation (Klaebe *et al*., 2017; Southgate, 1989).

For these reasons, dolomite in red siltstones was largely detrital, both eolian and fluvial, in contrast to marine cements in stromatolitic units. Clay enrichment near the surface is not in proportion to depletion in feldspar and rock fragments, and hydrolytic weathering within these beds would have been limited because of alkaline buffering by the abundant dolomite. Clay enrichment is more likely due to eolian delivery of clay in dust than by weathering in place, as seen in Quaternary soils of the clastic-poor Caribbean islands (Muhs *et al*., 1990; Muhs & Budahn, 2009). Clayey bed tops do not appear to be part of graded beds such as turbidites deposited in a water column (Komar, 1985; Korsch *et al*., 1993), for several reasons: little clay (Figure 7), no bedding (Figure 5), red colour (Figure 2f, g), and loess-like grainsize (Figure 6). Asymmetric enrichment of clay in bed tops over intervals of only 15 cm is unlike symmetrical hydrothermal or diffuse metamorphic alteration (Kelka *et al*., 2017; Wallace & Hood, 2018).

Chemical trends within beds

Chemical trends within the beds (Figure 7) are very different from those of graded beds such as turbidites, which show surface enrichment in alumina, lime and magnesia (Korsch *et al*.,1993). Uniformly low soda/potash ratios are evidence against soda enrichment (salinisation) within beds (Figure 7). Alkaline earths/alumina are high in proportion to the amount of silt-size dolomite clasts revealed by point counting. Variation in alumina/silica and alumina/bases are very modest within beds, and do not support the idea that clay in these profiles was created by hydrolytic weathering of feldspar and rock fragments. Ba/Sr molar ratios as evidence of chemical leaching are high in these dolomitic profiles, perhaps also supporting evidence from abundant detrital dolomite for limited silicate. Low ferrous/ferric iron confirms red colour from hematite as evidence of oxidising conditions, but rising ratios in the base of two beds may reflect chemical reduction (gleisation) within groundwater. Oxidation and reduction during the Tonian, rather than in modern outcrop, is indicated by alternation on scales of decimetres of drab and red beds in both outcrop and core extending for hundreds of metres (Figure 2). Oxidation only in outcrop is also disproved by identical red appearance in deep core (Figure 2b–d).

Molar weathering ratios do not show the sawtooth depth functions of chemically distinct interbeds of claystone and siltstone, but smooth and subdued trends are compatible with soil formation or massive deposition of relatively uniform beds (Figure 7). Such uniformity is common in paleosols derived from loess (Buggle *et al*., 2011; Prins *et al*., 2007), as also proposed here from grainsize analysis of the Johnnys Creek Formation (Figure 6).

Tau analysis

Analysed beds of the Johnnys Creek Formation show a mix of pedogenic and sedimentary alterations from the perspective of tau analysis (Figure 8). Modest enrichment in K, Fe^{3+}, Al and Mg in the Kwerralye profile only, perhaps from eolian dust input, as apparent from grainsize (Figure 6) and mineral trends (Figure 7). On the other hand, there are modest depletions of all elements in other beds, compromised by burial compaction. Nevertheless, there was limited chemical weathering and depletion of mass and weatherable elements (Figure 8), compatible with limited chemical differentiation of the beds (Figure 7).

Tau analysis (Brimhall *et al*., 1992) isolates two separate aspects of weathering: mole fraction mass transport ($\tau_{j,w}$) of a mobile element and mole fraction strain ($\varepsilon_{i,w}$) of an immobile element (Ti used here), using the formulae in Table 1. Soils and paleosols lose mass with weathering and so have negative strain ($\varepsilon_{i,w} < 0$), and also lose nutrient cations and silica, so have negative mass transfer ($\tau_{j,w} < 0$). In contrast, sediment accumulation and diagenetic alteration adds elements and mass so has positive strain and mass transfer. Negative strain due to soil formation is partly offset by burial compaction (Bestland *et al*., 1996; Retallack & Mindszenty, 1994). In sedimentary sequences, tau analysis of beds covers only the few decimetres between the sediment at the base of the bed as a parent material to the weathered top of the bed. Thus, tau analysis does not include weathering in hinterlands producing that sediment. Tau analysis has been widely used for Precambrian paleosols (Liivamägi *et al*., 2014; Retallack & Mindszenty, 1994), as well as Cenozoic paleosols (Bestland *et al*., 1996; Sheldon & Tabor, 2013), and modern soils (Chadwick *et al*., 1990; Hayes *et al*., 2019).

Stable isotopic covariance

The micritic low-magnesium, calcite nodules analysed here (Table 3) show strong covariance of $\delta^{13}C$ and $\delta^{18}O$ (Figure 9a). However, red dolomitic silt of the Johnnys Creek Formation in both Ellery Creek and core BR05 show a scatter with no correlation (crosses in Figure 9a). Low-magnesium calcite and dolomite in the Johnnys Creek Formation have very different origins.

Cross-plots of $\delta^{13}C$ and $\delta^{18}O$ in marine carbonate have long been used to screen for diagenetic alteration, including soil formation, karst weathering and methanogenic carbonate (Retallack, 2016). Unaltered marine limestones and sea shells (Figure 9e) show no hint of correlation (Surge *et al*., 1997; Veizer *et al*., 1999). The most profound early

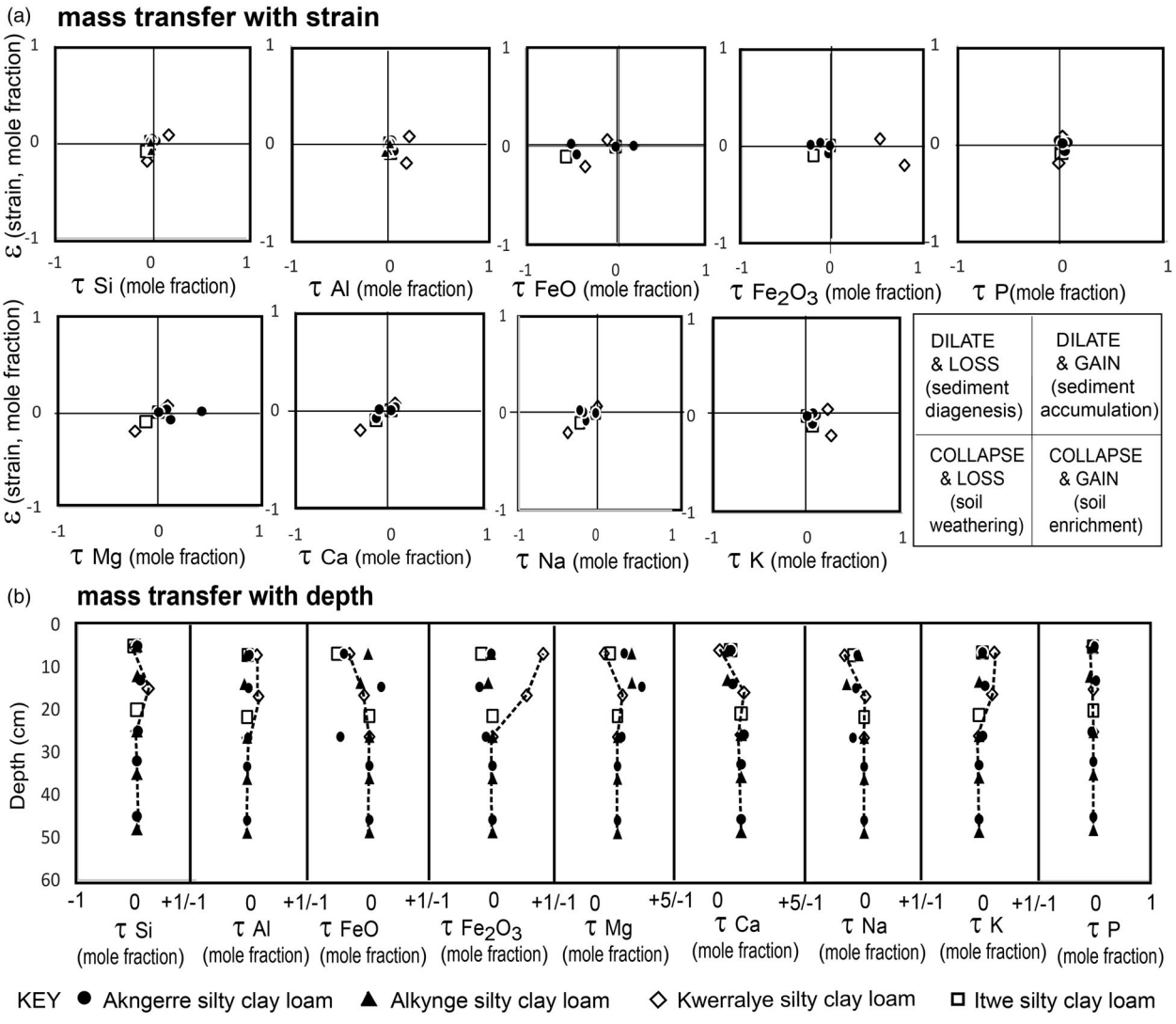

Figure 8. Tau analysis of paleosols from the Johnnys Creek Formation, including elemental mass transfer versus strain (a), and versus depth in paleosol profiles (b).

diagenetic alteration of carbonate is seen in pedogenic carbonate, which is an early diagenetic precipitation between deposition and burial of alluvial sediment (Retallack, 1991b, 2005). Thus, covariance is strong in Holocene soils (Figure 9b) in China (Huang *et al*., 2005) and Arizona (Knauth *et al*., 2003). Less statistically significant correlations (Figure 9c, d) are found in soil carbonate crusts (Knauth *et al*., 2003), and marine limestone altered by deep circulation of meteoric water (Lohmann, 1988; Melim *et al*., 2004). Lake carbonates with covariant stable isotopes may also be a case of meteoric alteration because covariance is only found in seasonally dry lakes, not perennial open system lakes (Talbot, 1990). Near constant $\delta^{18}O$ but highly varied $\delta^{13}C$ (Figure 9f) is created by microbial methanogenesis in carbonate of marine methane seeps (Aiello *et al*., 2001; Peckmann *et al*., 2002), and siderite of wetland paleosols (Ludvigson *et al*., 1998, 2013).

From this perspective, the low-magnesium calcite nodules in the Johnnys Creek Formation have isotopic covariance like pedogenic nodules, but dispersed dolomite is uncorrelated like marine dolostones. This evidence supports the idea from granulometry (Figure 6) and mineral weathering (Figure 7) that the silt-sized dolomite is not pedogenic, but loess derived from physical erosion of marine dolostones like associated stromatolitic dolostones of the lower Bitter Springs Group (Swanson-Hysell *et al*., 2012).

Tight correlations of $\delta^{13}C$ and $\delta^{18}O$ are not accidental, but due to selection for light isotopologues of CO_2 in soils (Broz *et al*., 2021; Farquhar & Cernusak, 2012), unlike the sea or lakes with oxygen of water vastly in excess of carbon (Retallack, 2016). Correlation may be due to kinetic evaporative effects in narrow spaces of soils (Ufnar *et al*., 2008), to stomatal conductance, and to fractionation by enzymes such as rubisco (Retallack, 2016) and carbonic anhydrase (Chen *et al*., 2018). Stomata and enzymes are supported by $\delta^{13}C$ and $\delta^{18}O$ covariance in respired soil CO_2 (Ehleringer *et al*., 2000; Ehleringer & Cook, 1998), and in

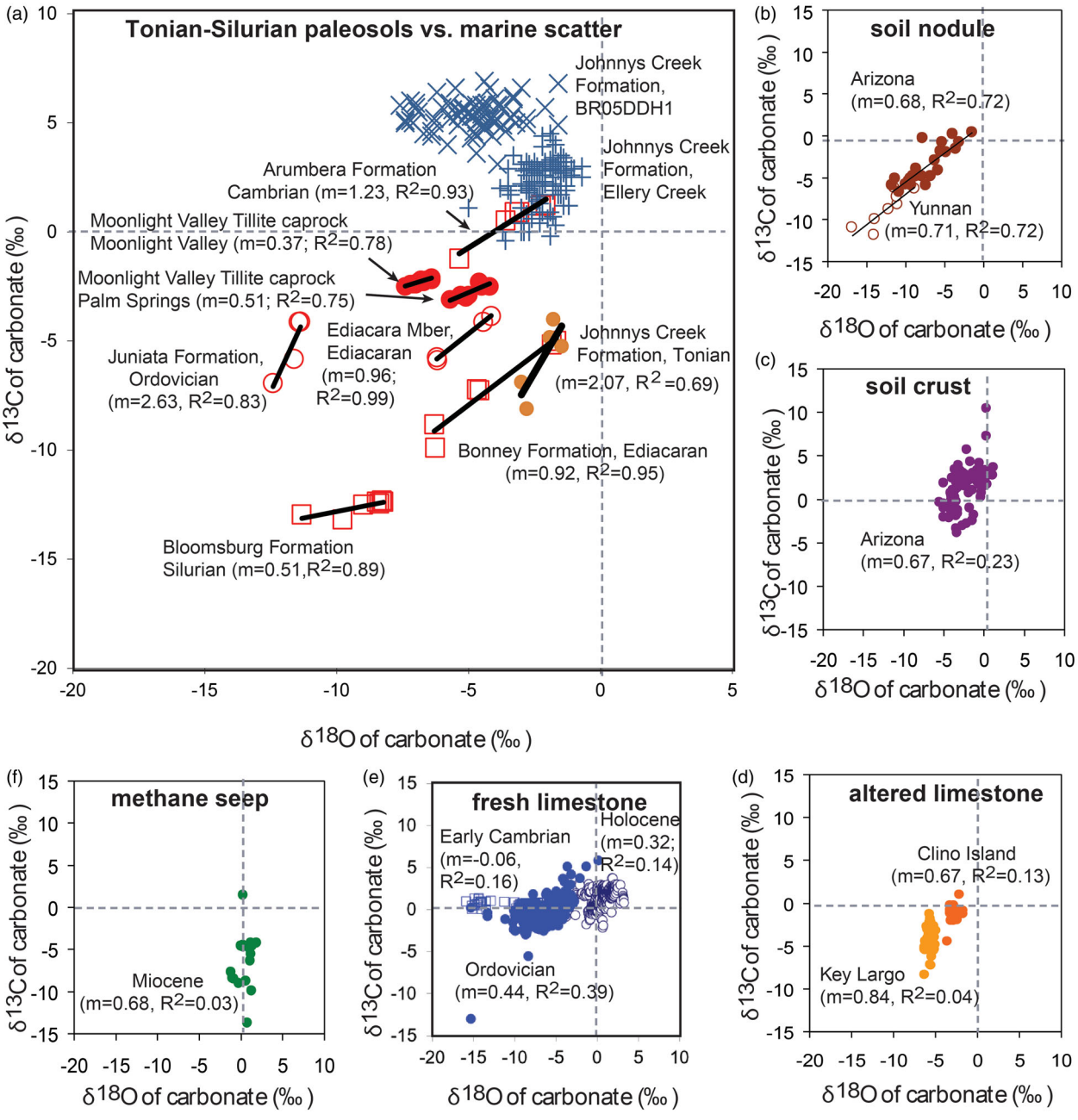

Figure 9. Covariance of carbon and oxygen isotopic composition of carbonate as a characteristic of paleosols, rather than other settings: (a) Tonian Johnnys Creek Formation (Table 3), early Ediacaran cap carbonate of Moonlight Valley Tillite at two localities (Bao *et al.*, 2012), Ediacaran paleosols of South Australia (Retallack *et al.*, 2014), Cambrian Arumbera Formation at Ross River (Retallack & Broz, 2020), Ordovician paleosols of Pennsylvania (Retallack, 2015a), and Silurian paleosols of Pennsylvania (Retallack, 2015b); (b) soil nodules (above Woodhouse lava flow, near Flagstaff, Arizona (Knauth *et al.*, 2003) and in Yuanmou Basin, Yunnan, China (Huang *et al.*, 2005); (c) soil crusts on basalt (Sentinel Volcanic Field, Arizona, from Knauth *et al.*, 2003); (d) Quaternary marine limestone altered diagenetically by meteoric water (Key Largo, Florida, Lohmann, 1988, and Clino Island, Bahamas, Melim *et al.*, 2004); (e) Holocene (open circles) and Ordovician (open squares) unweathered marine limestones (Veizer *et al.*, 1999) and early Cambrian (closed circles), Ajax Limestone, South Australia (Surge *et al.*, 1997); and (f) marine methane cold seep carbonate (Miocene, Santa Cruz Formation, Santa Cruz, California (Aiello *et al.*, 2001). Slope of linear regression (m) and coefficients of determination (r^2) show that carbon and oxygen isotopic composition is significantly correlated in soils and paleosols, but not in other settings.

plant cellulose (Barbour *et al.*, 2002; Barbour & Farquhar, 2000). A role for stomates is undermined by correlation of $\delta^{13}C$ and $\delta^{18}O$ in early Paleozoic and Ediacaran paleosols because they predate the evolution of stomates, so enzymatic control is more likely responsible for observed covariance in Precambrian pedogenic carbon (Figure 9). The covariance is neither destroyed nor enhanced by metamorphism to greenschist facies in paleosols of the Juniata and Bloomsburg formations (Retallack, 2015b, 2015c).

Table 4. Pedotypes and diagnosis for Tonian red beds of central Australia.

Pedotype	Meaning	Diagnosis	USDA (Soil Survey Staff, 2014)	FAO (1977, 1978)	Classic (Stace *et al.*, 1968)	Australian (Isbell, 1996)
Akngerre	Big	Cracked red siltstone (A) surface over red siltstone with calcite nodules (Bk).	Calcid	Calcic Xerosol	Calcareous Brown Earth	Hypercalcic Calcarosol
Alkynge	Eye	Cracked red siltstone (A) surface over red siltstone with gypsum sand crystals (By).	Gypsid	Orthic Solonchak	Red Desert Soil	Red Sodosol
Kwerralye	Star	Cracked red siltstone (A) surface over clayey red siltstone (Bw).	Ochrept	Dystric Cambisol	Brown Earth	Brown-orthic Tenosol
Itwe	Near	Cracked red clayey siltstone (A) bedded red sandstone (C).	Fluvent	Dystric Fluvisol	Alluvial Soil	Stratic Rudosol

Indigenous names for pedotypes are from Arrernte language (Broad, 2008).

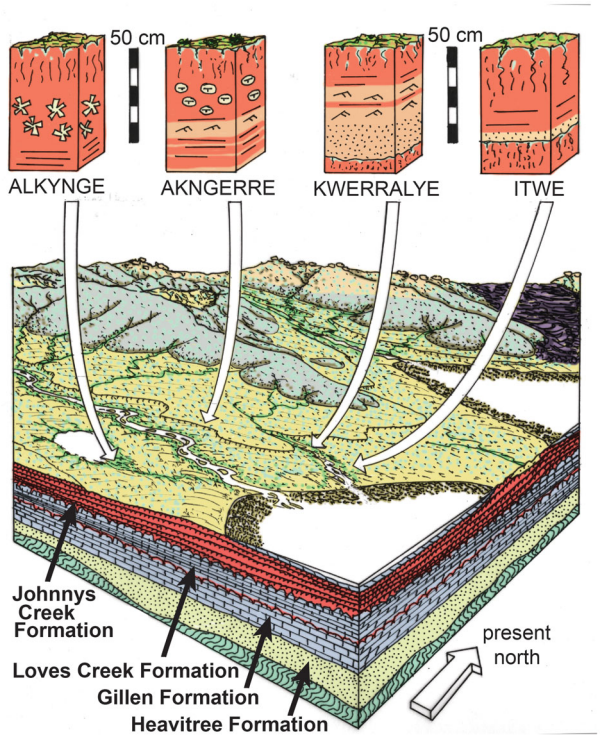

Figure 10. Reconstructed Tonian soils of the Johnnys Creek Formation, central Australia.

Paleosol interpretation

Paleosol classification

The preceding paragraphs described a variety of paleosol features in the Johnnys Creek Formation, but the rest of this paper explores the kinds of paleosols present and their paleoenvironmental implications. The various kinds of beds analysed as putative paleosols have been given non-genetic names (Table 4) using the Arrernte (sometimes transliterated 'Aranda' or 'Arunta') aboriginal language (Broad, 2008). These pedotypes can be interpreted in terms of soil taxonomy and various soil-forming factors to build a detailed model of their paleoenvironment (Figure 10). Alkynge profiles with cracked surface (A horizon) over a diffuse horizon with mottles and sand crystals (By or gypsic) are most like Gypsids (Soil Survey Staff, 2014). Akngerre profiles, on the other hand, have cracked surfaces (A horizon) over a deep horizon (Bk or calcic) of pedogenic carbonate nodules, as in Calcids (Soil Survey Staff, 2014). The same criteria can be used to classify these paleosols in other classifications (Table 4) of Australia (Isbell, 1996; Stace *et al.*, 1968), and of the Food and Agriculture Organization (1978). Other profiles, of Kwerralye and Itwe pedotypes, are less well developed Entisols and Inceptisols (of Soil Survey Staff, 2014), and would have been restricted to disturbed parts of the landscape (Table 5).

In the FAO map classification (Food & Agriculture Organization, 1978) the Alkynge pedotype of the lower Johnnys Creek Formation was Orthic Solonchak and would represent a map code of Zo + Jd,Gd (Table 4). The closest modern match is map unit Zo36–2a + Rd,Rc,Xk,Yh in hot desert around Lake Mackay and other alluvial and playa plains on the border of Northern Territory and Western Australia (Food & Agriculture Organization, 1978). At nearby Walungurru Airport, mean annual temperature is 26.2 °C and mean annual precipitation is 280 mm (Bureau of Meteorology, 2020). The calcareous Akngerre pedotype were Calcic Xerosols, in a map code Xk + Rc, most like Xk45–21 + Rc similar to the coastal plain inland of Eighty Mile Beach in the northwest coast of Australia (Food & Agriculture Organization, 1978). At nearby Mandora, mean annual temperature is 26.8 °C and mean annual precipitation is 378 mm (Bureau of Meteorology, 2020). Similar soils also form in cooler climates. Hypercalcic Calcarosols similar to Akngerre paleosols have formed on an alluvial plain near Clare, South Australia, under mean annual precipitation of 444 mm, and mean annual temperature of 15.2 °C (profile CA7 of McKenzie *et al.*, 2004). Red Sodosols similar to Alkynge paleosols formed on an alluvial plain near Deniliquin, New South Wales, under mean annual precipitation of 339 mm and mean annual temperature of 15.7 °C (profile SO3 of McKenzie *et al.*, 2004). These modern comparisons provide a general idea of Tonian paleoenvironments, but the following evaluates each of these interpretations in detail.

Table 5. Interpretation of pedotypes for Tonian red beds of central Australia.

Pedotype	Paleoclimate	Ecosystems	Parent materials	Paleo-topography	Time for formation (yrs)
Akngerre	Cool temperate (mean annual temperature 6.6 ± 4.4 °C), arid (mean annual precipitation 291 ± 147 mm), seasonal (mean annual range of precipitation 41 ± 22 mm)	Polsterland dominated with cyanobacteria, actinobacteria, fungi and algae	Dolomitic loess	Well-drained floodplain	5900 ± 4800
Alkynge	Cool temperate (Mean annual temperature 6.2 ± 4.4 °C), hyperarid (mean annual precipitation 142 ± 129 mm)	Microbial earth dominated by cyanobacteria and actinobacteria	Dolomitic loess	Well-drained floodplain	47 400 ± 15 000
Kwerralye	Not diagnostic for climate	Early successional microbes	Dolomitic loess	Alluvial levee	<1000
Itwe	Not diagnostic for climate	Early successional microbes	Dolomitic loess	Near-stream	<100

This table is a summary of five interpretive sections of text.

Original parent material

Parent materials to paleosols of the Johnnys Creek Formation were largely dolomitic loess (Figures 6 and 7). This parent material has isotopically enriched $\delta^{13}C$ values (Figures 3 and 4), uncorrelated with $\delta^{18}O$ (Figure 9), so derived from a marine dolostone by eolian or glacial erosion. Its carbonate $\delta^{13}C$ values are much higher than that of the underlying Loves Creek Formation but could have been derived from physical erosion of the Gillen Formation of the Bitter Springs Group (Swanson-Hysell *et al*., 2012). The Gillen Formation includes thick halite units that were deformed by salt tectonics before deposition of the overlying Loves Creek Formation (Lindsay, 1987). Such highly positive $\delta^{13}C$ values are widely found in Precambrian red-bed dolomite successions of intracratonic playa lakes, perhaps due to enrichment by evaporation or methanogenic degassing of very light carbon (Melezhik *et al*., 1999). Clay may also have been included in this eolian parent material because there is little evidence for clay production in the profile from abundance of weatherable minerals or alumina/silica or alumina/bases ratios (Figure 7), as in soils near the arid-hyperarid transition in Chile (Ewing *et al*., 2006). Loess plains are among the most productive of modern soil parent materials, rich in weatherable minerals and physically stable (Fehrenbacher *et al*., 1986; Swineford & Frye, 1951).

Reconstructed sedimentary setting

Detrital zircon age spectra of the Johnnys Creek Formation are evidence of a source terrane to the north in the Aileron and Warumpi basement provinces (Kositcin *et al*., 2015). These were hills of granites and schists formed during the Paleoproterozoic (1880–1590 Ma: Zhao & Bennett, 1995). Low ridges of Gillen Formation deformed by salt tectonics also flanked the depositional basin to the immediate north during deposition of the Johnnys Creek Formation (Lindsay, 1987). Continental tholeiitic basalts in the Johnnys Creek Formation in the northeastern part of the Amadeus Basin would have had low relief, like other flood basalts (Barovich & Foden, 2000; Zhao *et al*., 1994). Trace elements in stromatolites of the Johnnys Creek Formation are light-REE-enriched unlike fully marine stromatolites, and comparable with continent-margin fringing reefs, rather than open seawater (Corkeron *et al*., 2012). Such a setting of a restricted arm of the ocean in an area of subdued relief is similar to modern stromatolites of Hamelin Pool in Shark Bay, Western Australia, within the intertidal zone below the beach and coastal plain (Cockbain, 1976). Open ocean was toward the southeast of Ellery Creek during the Tonian (Scotese, 2009).

Grainsize distribution (Figure 6), mineral contents (Figure 7), and angularity of Johnnys Creek siltstones are comparable with modern loess (Bettis *et al*., 2003; Pye & Sherwin, 1999; Swineford & Frye, 1951). Loess plains form distinctive land forms best characterised as 'rolling downs' (Figure 10), but with steep angle of repose of terraces and erosional gullies near streams because of their angular silt grains (Zakrzewska, 1963). Relief during accumulation of the Johnnys Creek Formation would have been low to allow sequential transgression of marine-influenced stromatolitic limestones, but the loess plain itself was well drained with little indication of waterlogging (gleisation; Figure 7) for Akngerre and Alkynge paleosols. Gleisation low within Kwerralye and Itwe profiles may have been due to a high water-table. These lowland paleosols may have formed near streams for Itwe and on alluvial levees for Kwerralye paleosols.

Time for formation

The time over which individual paleosols form gives information on sediment accumulation rates of sequences of paleosols. Duration of soil formation for Alkynge and Akngerre pedotypes can be calculated from

chronofunctions for modern arid-land soils. Diameter of pedogenic-carbonate nodules (*D* in cm) is related to radiocarbon age of nodules (A in kyrs) near Las Cruces, New Mexico (Retallack, 2005), using an equation in Table 1. Similarly, abundance of gypsum in a profile (*G* as % surface area using comparison chart of Terry & Chilingar, 1955) is a metric for age (*A* in kyrs) in the Negev Desert of Israel (Retallack, 2013a), according to the equation in Table 1.

The New Mexico calcic chronofunction applied to 290 Akngerre paleosols in core BR05 gives durations of 3.3 ± 1.8 kyr at a depth of 974.4 m ranging up to 13.2 ± 1.8 kyr at a depth of 556.4 m. Means and standard deviation for durations of all 290 paleosols are 5.9 ± 4.8 kyr. Similarly, 31 Akngerre paleosols exposed in Ellery Creek have durations of 2.2 ± 1.8 kyr at a level of 428.5 m ranging up to 4.9 ± 1.8 kyr at a level of 672.9 m. Means and standard deviation for durations of all 31 paleosols in Ellery Creek are 2.6 ± 0.9 kyr. The Negev gypsic chronofunction applied to 100 Alkynge paleosols in core BR05 gives durations of 53.6 ± 15 kyr at a depth of 1068.3 m to 41.6 ± 15 kyr at a depth of 541.0 m. Means and standard deviation for durations of all 100 paleosols are 47.39 ± 14.9 kyr. Similarly, 6 Alkynge paleosols exposed in Ellery Creek have durations of 37.7 ± 15 kyr at a level of 382.0 m ranging up to 21.7 ± 15 kyr at a level of 427.2 m. Means and standard deviation for durations of all six paleosols in Ellery Creek are 35.0 ± 9.5 kyr. These Tonian paleosols are thus moderately developed, in the usual scale in which Holocene (up to 10 kyr) soils are moderately developed (Retallack, 2019). The calcic Akngerre profiles show increasing duration up section, and thus lower sediment accumulation rate, in both core and outcrop, but the gypsic Alkynge palesols show no significant change in sediment accumulation rate. This slowing of sediment accumulation rate in the upper Wallara Formation culminated with sea-level fall and erosion of paleovalleys some 200 m deep before deposition of Areyonga Formation tillites in Ellery Creek (Lindsay, 1989).

Other paleosols would have been much less developed, with a few millennia likely for Kwerralye paleosols with sedimentary structures obscured to a depth of 21 cm, and a century or less for Itwe paleosols with clear relict bedding. These are maximal estimates, because based on comparison with homogenisation of bedding in Pleistocene soils of the San Joaquin Valley, California (Harden, 1982), which were more actively rooted and burrowed than Tonian soils. Given these biotic differences, the observed homogenisation of Tonian paleosols is impressive. Similar Tonian paleosols in Arizona, USA, were homogenised by fungal hyphae and rope-forming cyanobacteria (Retallack *et al*., 2021).

Paleoclimate

Gypsic and calcic horizons are today found at depths in soils proportional to mean annual precipitation (Retallack, 2005; Retallack & Huang, 2010). Calcic soils are widespread in arid lands, but gypsic soils form in extreme deserts such as the Atacama Desert of Chile (Ewing *et al*., 2008; Navarro-González *et al*., 2003). For calcic paleosols, mean annual precipitation is related to depth in the profile to calcareous nodules corrected for burial compaction from a global compilation (Retallack, 2005), following the equation in Table 1. For gypsic soils, another global compilation gives mean annual precipitation from depth to gypsum, again compaction corrected (Retallack & Huang, 2010), using the equation in Table 1. Seasonality of precipitation, defined as wettest minus driest month mean precipitation, is a function of thickness of the calcic horizon, again from a global compilation (Retallack, 2005). In highly seasonal climate, carbonate precipitates at a wide range of levels within soil profiles.

The calcic climofunction applied to 290 Akngerre paleosols in core BR05, corrected for compaction using an equation in Table 1, gives paleoprecipitation of 231 ± 147 mm at a depth of 974.4 m to 361 ± 147 mm at a depth of 556.4 m. Means and standard deviation for paleoprecipitation of all 290 paleosols are 291 ± 40 mm. Similarly, 31 Akngerre paleosols exposed in Ellery Creek yield paleoprecipitation of 309 ± 147 mm at a level of 428.5 m ranging up to 243 ± 147 mm at a level of 672.9 m (Figure 3h). Mean and standard deviation for paleoprecipitation of all 31 paleosols in Ellery Creek is 288 ± 39 mm.

The gypsic climofunction applied to 100 Alkynge compaction-corrected paleosols in core BR05 gives paleoprecipitation of 135 ± 129 mm at a depth of 1068.3 m to 216 ± 129 mm at a depth of 541.0 m. Means and standard deviation for paleoprecipitation of all 100 paleosols are 142 ± 22 mm. Similarly, 6 Alkynge paleosols exposed in Ellery Creek yield paleoprecipitation of 125 ± 129 mm at a level of 382.0 m ranging up to 135 ± 129 mm at a level of 427.2 m. Means and standard deviation for paleoprecipitation of all six paleosols in Ellery Creek are 143 ± 22 mm.

These Tonian paleosols are thus hyperarid near the base of the Johnnys Creek Formation, where there are numerous gypsic paleosols (Alkynge) like those of the modern Atacama Desert (Ewing *et al*., 2006, 2008; Navarro-González *et al*., 2003). By the top of the Johnnys Creek Formation climate was arid to semiarid, with calcic paleosols (Akngerre), and deeper calcic horizons. A similar transition from gypsic to calcic paleosols during the late Tonian has also been documented in the Grand Canyon, Arizona (Retallack *et al*., 2021).

Seasonality of precipitation, or wettest month average minus driest month average (±22 mm), for 290 Akngerre paleosols in core BR05 gives 41 ± 10 mm and for 31 Akngerre paleosols exposed in Ellery Creek yield 37 ± 3 mm, and both are modest, non-monsoonal seasonalities (Retallack, 2005).

A variety of pedogenic paleothermometers based on modern soils (Gallagher & Sheldon, 2013; Óskarsson *et al*., 2012) gave frozen temperatures, because of the unusually dolomitic parent material of paleosols in the Johnnys Creek

Formation. A paleothermometer based on modern soils, which does not use lime is alkali index (Sheldon *et al*., 2002), which predicts mean annual temperature from the ratio of soda + potash/alumina (Table 1). This chemical proxy gives mean annual temperature of 4.9 ± 4.4 °C for the lower A horizon of the Akngerre silty clay loam paleosol and 4.3 ± 4.4 °C for the lower A horizon of the Alkynge silty clay paleosol. An additional six Alkynge profiles in BR05 core yielded paleotemperatures of 6.2 ± 1.0 °C, and 15 Akngerre profiles in BR05 core gave paleotemperature 6.6 ± 1.1 °C. These are all cold temperate climates, compatible with loess deposition and the coeval (752.1 Ma) Konnarock Glaciation of Virginia, USA (MacLennan *et al*., 2020). Cool paleotemperatures are surprising considering subtropical paleolatitude of 26.2° from hematite of the Johnnys Creek Formation, which appears original, unlike later remagnetised pyrrhotite and magnetite in the underlying Loves Creek Formation (Swanson-Hysell *et al*., 2012). Paleolatitudes calculated using formulae of Butler (1992) and Haile (1975) did not appreciably change during accumulation of the Johnnys Creek Formation (Figure 3j).

Finally, atmospheric CO_2 can be calculated from the isotopic composition of pedogenic carbonate in Akngerre paleosols, and other data in Table 3. Diagenetic alteration of original pedogenic carbonate isotopic composition is ruled out by high correlation of carbon and oxygen isotope values in low-magnesium calcite nodules, comparable with modern soils (Figure 9), and also by unrecrystallised, micritic grainsize in thin-section (Figure 5). This analysis excluded data from dolomite rhombs regarded as eolian (Figure 6). The CO_2 paleobarometer of Cerling (1991) estimates past atmospheric CO_2 (P_a in ppmv) from the balance within soils at the depth of carbonate nodules between isotopically light soil CO_2 ($\delta^{13}C_s$) compared with isotopically heavy atmospheric CO_2 ($\delta^{13}C_a$), as refined for paleoproductivity effects (Breecker & Retallack, 2014). A variety of terms in the governing equation are derived from other analyses and transfer functions, shown in Table 1. The isotope value of soil CO_2 ($\delta^{13}C_s$) comes from that of pedogenic carbonate ($\delta^{13}C_c$) and temperature (T in °C) at the time of precipitation (Romanek *et al*., 1992). The isotope value of associated soil organic matter ($\delta^{13}C_o$), provided for the Bitter Springs Group by Swanson-Hysell *et al*. (2010), is used as a proxy for respired soil CO_2 ($\delta^{13}C_r$) and also to calculate the isotope value of atmospheric CO_2 ($\delta^{13}C_a$; Fletcher *et al*., 2005). Finally, partial pressure of respired CO_2 in soil (P_r) is from its known relationship with depth to carbonate nodules (D_o, corrected for compaction in paleosols) in modern soils (Breecker & Retallack, 2014). Some of this respired CO_2 in desert soils studied by Cerling (1991) is from root respiration, but most of it in soil pores beyond the rhizosphere is from microbial respiration (Monger *et al*., 1991), allowing use of these proxies for pre-Devonian paleosols.

These equations can be used to calculate atmospheric soil CO_2 and other components of that calculation for the five calcic (Akngerre) paleosols analysed are presented in Table 3 and plotted in Figure 4j. Values of 1320–1750 ppm are 4.7–6.2 times preindustrial atmospheric level of 280 ppm and are very similar to other estimates of Proterozoic CO_2 derived from a different mass balance model (Sheldon, 2006). Values this high produced dangerously high temperatures during the past 300 million years (Retallack & Conde, 2020), but were not so severe 785–717 Ma when solar luminosity was only 94% of modern levels (Feulner, 2012)

Life on land

Aquatic fossil stromatolites of the Bitter Springs Group were lacustrine or marine intertidal from their sedimentary setting (Southgate, 1989, 1991) and trace-element chemistry (Corkeron *et al*., 2012). Microfossils in silicified stromatolites have been interpreted as prokaryotic cyanobacteria, eukaryotic green algae, and possible fungi (Oehler, 1976, 1977; Schopf, 1968; Schopf & Blacic, 1971). *Eomycetopsis* as fungal hyphae rather than cyanobacterial sheaths have been doubted for lack of fossils of reproductive structures (Knoll & Golubic, 1992), but fungal spores are now known well back into the Proterozoic (Loron *et al*., 2019; Retallack, 2015c). Also found in the Bitter Springs Group were biomarkers for cyanobacteria such as 2α-methyl hopanes (Brocks *et al*., 1999; Summons & Walter, 1990), and for algae such as C_{30} desmethyl steranes and 4-methylsteranes (Hill *et al*., 2000). Cholestane biomarkers for C_{27} cholesterol in the Johnnys Creek and Wallara formations preceded Ediacaran sterane diversification (Brocks *et al*., 2017), and could represent red algae, fungi, or metazoans (Bobrovskiy *et al*., 2018; Retallack & Broz, 2020).

Cyanobacteria, unicellular algae and fungi now thrive on land in biological soil crusts (Belnap, 2003), but evidence for them is indirect in the Johnnys Creek Formation red bed paleosols. Thin-sections show lack of lamination in paleosol surface horizons (Figures 3 and 5f, g), perhaps due to vertical thread-forming microbial consortia and fungal hyphae (Retallack, 2012). The paleosols also show 2–5 wt% (0.02–0.05 mole fraction) surficial depletion of phosphorus (Figure 8), another indication of a microbial earth soil (Neaman *et al*., 2005a, 2005b).

Depth to gypsic and calcic horizons, corrected for burial compaction are proxies for soil-respired CO_2 (Breecker & Retallack, 2014), using separate equations for calcic and gypsic horizons (Table 1). This secondary productivity of CO_2 can be as high as 104 000 ppm in modern soils, and controls the level at which soluble salts can be precipitated in the soil, and is also related to mean annual precipitation. The calcic productivity metric applied to 290 Akngerre paleosols in core BR05 gives 1122 ± 768 ppm soil-CO_2 at a core depth of 974.4 m to 1914 ± 768 mm at a depth of 556.4 m (Figure 4i). Means and standard deviation for soil-CO_2 of all 290 paleosols are 1476 ± 246 ppm. Similarly, 31 Akngerre paleosols exposed in Ellery Creek yield soil-CO_2 of

1187 ± 768 ppm at a level of 428.5 m ranging up to 1583 ± 768 ppm at a level of 672.9 m (Figure 3i). Mean and standard deviation for soil-CO_2 of all 31 paleosols in Ellery Creek is 1461 ± 235 mm. Although the depths to Bk are significantly greater higher in the section, the high standard deviation of the transfer function does not make this a significant difference in paleoproductivitiy. The gypsic productivity metric applied to 100 Alkynge paleosols in core BR05 gives soil-CO_2 of 1292 ± 552 ppm at a depth of 1068.3 m to 2252 ± 552 ppm at a depth of 541.0 m. Means and standard deviation for soil-CO_2 of all 100 paleosols are 1371 ± 291 ppm. Similarly, 6 Alkynge paleosols exposed in Ellery Creek yield soil-CO_2 of 1128 ± 552 ppm at a level of 382.0 m ranging up to 1290 ± 552 ppm at a level of 427.2 m. Means and standard deviation for soil-CO_2 of all six paleosols in Ellery Creek are 1134 ± 283 kyr. These are significant differences in both depth and productivity of gypsic paleosols through time. In each section, both calcic and gypsic paleosols indicate an increase in soil-respired CO_2 during deposition of the Johnnys Creek Formation. Given static paleolatitude (Figure 3j) and very slight decrease in atmospheric CO_2 (Figure 4j) over this same interval, soil productivity was increasing due to soil biology rather than continental drift or climate change.

Increased productivity through time is also apparent in the transition from gypsic (Alkynge) paleosols near the base of the section to mainly calcic (Akngerre) paleosols with only a few gypsic paleosols near the top (Figures 3 and 4). A similar Tonian gypsic to calcic transition has been demonstrated in the Grand Canyon, Arizona (Retallack *et al*., 2021). A comparable community transition and its microbiome has been studied in the Atacama Desert of Chile, where gypsic soils of the hyperarid valley bottom playas pass upward to calcic soils of semiarid slopes (Quade *et al*., 2007; Rech *et al*., 2003). Hyperarid gypsic soils have low overall diversity dominated by cyanobacteria and actinobacteria, but semiarid calcic soils have greater diversity, including fungi, archaea, algae, bunch grass and saltbush (Araya *et al*., 2020; Castillo & Beck, 2012; Neilson *et al*., 2012, 2017; Quade *et al*., 2007; Vítek *et al*., 2013). Much of the biota of hyperarid gypsic soils is dormant and comes to life only after rare rains (Crits-Christoph *et al*., 2013). Lichens aid formation of carbonate in calcic soils from excretion of precursor oxalate (Giordani *et al*., 2003; Verrecchia *et al*., 1993; Vítek *et al*., 2013). Another modern analogue for transition from cyanobacterial to lichen communities is ecological succession in western North American desert soil crusts, which show the following stages: (1) bare soil; (2) large filamentous cyanobacteria such as *Microcoleus vaginatus*; (3) gelatinous lichens such as *Collema coccophorum*; (4) squamulose lichens such as P*sora cerebriformis*; (5) crustose lichens such as *Diploschistes scruposus*; (6) liverworts such as *Cephaloziella divaricata*; (7) short mosses such as *Bryum argenteum*; (8) foliose lichens such as *Xanthoparmelia convoluta*; (9) tall mosses such as *Syntrichia ruralis*; (10) fruticose lichens such as *Aspicilia filiformis*; (11) early successional angiosperms such as *Chrysothamnus nauseus*; and (12) late successional angiosperms such as *Artemisia tridentata* (Belnap *et al*., 2001; Rosentreter, 1984). The gypsic-calcic transition in the Johnnys Creek Formation may reflect evolution to successional stage five by the late Tonian, as in a comparable paleosol sequence in Arizona, USA (Retallack *et al*., 2021), with land plants evolving perhaps by Cambrian (Strother *et al*., 2017).

Plausible megafossils were discovered in the Johnnys Creek Formation in Ellery Creek during the course of this work (Figure 11), but collections remain too meagre for formal description. All except one from laminated shale at 494 m (Figure 11a) were found atop an Akngerre paleosol at 440 m in the section (Figure 3). They are briefly characterised here as search images for the future, and as preliminary evidence for the kind of vegetation called a polsterland, with scattered megascopic clumps (Retallack, 1992). Some of the newly discovered fossils may have been aquatic algae (Figure 11a), with segmented stems comparable with charophytes (McCourt *et al*., 2004). Algae of comparable size are known in Cryogenian rocks elsewhere, such as *Chingiskaania bifurcata* (Dornbos *et al*., 2016). Other fossils are surface markings widely known as microbially induced sedimentary structures (MISS of Noffke, 2010). These can be non-marine if they show healed cracks like the well-known 'old elephant skin' (Retallack & Broz, 2020), but many MISS are undulose and aquatic (Breyer *et al*., 1995; Noffke, 2010). A variety of trace fossil names are available for such microbially textured surfaces (Neraudeau *et al*., 2018; Stimson *et al*., 2017), but this example (Figure 11b) appears to be an aquatic form, *Neantia reticulata* (Lebesconte, 1887). Also similar are enigmatic flaring structures from the 1.1 Ga Copper Harbor Formation of Michigan (Anderson *et al*., 2016). Discoid fossils are known in many mud-cracked red beds as ancient as Paleoproterozoic (Grazhdankin *et al*., 2012; Hofmann *et al*., 1990; Meert *et al*., 2011; Retallack & Mao, 2019; Serezhnikova *et al*., 2014), and are likely to have been microbial colonies (Grazhdankin & Gerdes, 2007). The example found in the Johnnys Creek Formation (Figure 11c) has fine radial lineation like *Medusinites asteroides* (Sprigg) Glaessner and Wade (1966). Small areas of quilted surface are most like Ediacaran fronds of enigmatic biological affinities, perhaps lichens, fungi, stem metazoan, or cnidarians, attributed to the problematic Class Vendobionta (Retallack & Broz, 2020). The single specimen from Ellery Creek with fractally organised quilts (Figure 11d), is most like frond-like forms such as *Beothukis* (Taylor *et al*., 2019), *Avalofractus* (Narbonne *et al*., 2009), and *Trepassia* (Retallack & Broz, 2020). Faint tapering trails with levees, backfills and central groove (Figure 11e, f) are similar to *Lamonte trevallis* (Meyer *et al*., 2014). Although attributed to activity of a wormlike metazoan (Meyer *et al*., 2014), that explanation does not explain their tapering. Another hypothesis is that they were formed by the grex phase of

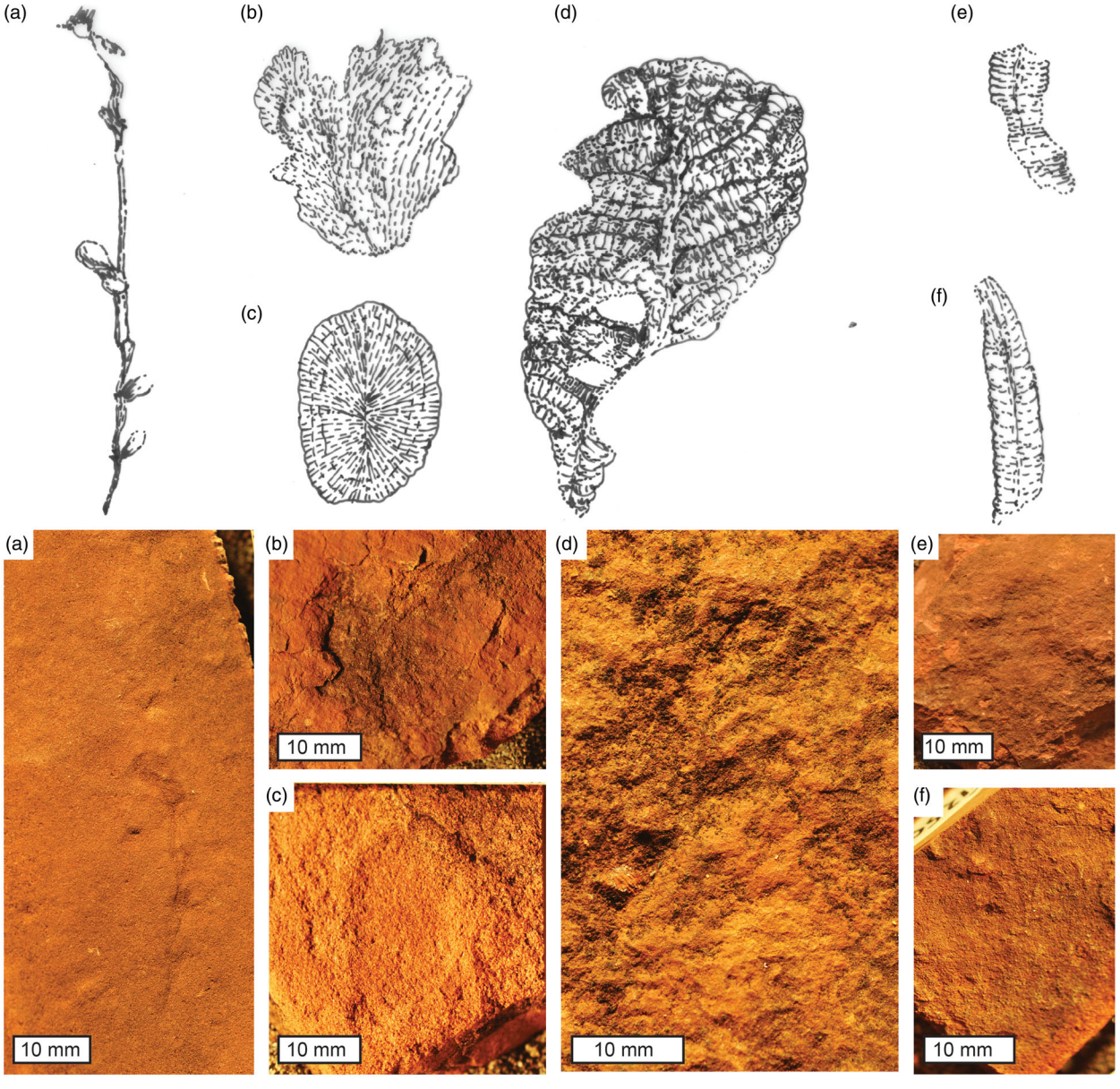

Figure 11. Megafossils from the Johnnys Creek Formation in Ellery Creek, with interpretive sketches: (a) possible charophyte alga; (b) *Neantia reticulata* Lebesconte, 1887, microbially textured surface; (c) *Medusinites asteroides* (Sprigg) Glaessner & Wade, 1966, microbial colony impression; (d) fractal quilted structure, comparable with vendobiont fronds; and (e, f) *Lamonte trevallis* Meyer *et al.* (2014), likely social amoebae trail. Specimens are in the Museum of Natural and Cultural History of the University of Oregon, Eugene: (a) F125033; (b) F125028; (c) F119679; (d) F125031; (e) F125032; (f) F119679.

social amoebae (dictyostelid Mycetozoa), aggregating to move to a new position for sporulation (Retallack & Broz, 2020). Testate amoebae are known from Tonian rocks elsewhere (Porter *et al.*, 2003; Porter & Knoll, 2000). Other plausible megafossils from the underlying Heavitree Formation (Lindsay, 1991) and overlying Areyonga Formation (Wells *et al.*, 1967), may be ice wedges (Kokelj *et al.*, 2007; Raffi & Stenni, 2011) and rollups (Beraldi-Campesi & Retallack, 2016; Noffke, 2010), respectively. Life on land during the late Tonian may not have been entirely microscopic.

What, if anything, is a 'cap carbonate'?

Terminating 'Snowball Earth' glacial expansion, according to a popular theory (Hoffman & Li, 2009; Hoffman & Schrag, 2002; Kasemann *et al.*, 2014; Yu *et al.*, 2020), were volcanogenic greenhouse spikes causing oceanic alkalisation events inferred from 'cap carbonates', which are isotopically anomalous dolomites and limestones overlying tillites. The unusually depleted $\delta^{13}C$ values of these carbonates have been used as time markers through the Neoproterozoic (Corkeron, 2007, 2008; Halverson *et al.*, 2010; Swanson-Hysell *et al.*, 2012). One idea is that

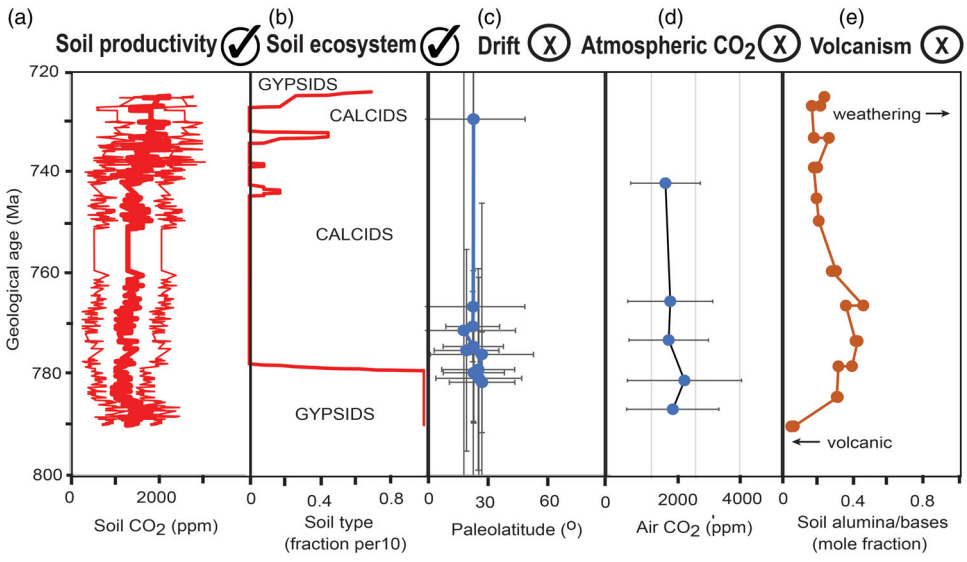

Figure 12. Comparison of critical pre-Cryogenian time series from two sections (Figures 3 and 4) of the Johnnys Creek Formation of central Australia converted to age models (Table 1): (a) soil productivity as ppm CO_2 (using method of Breecker & Retallack, 2014); (b) transition from Gypsic to Calcic paleosols as fraction of 10 point running mean; (c) paleolatitude of the Johnnys Creek Formation (data of Swanson-Hysell *et al.*, 2012); (d) atmospheric CO_2 (using method of Breecker & Retallack, 2014); and (e) molar ratio of alumina/bases in BR05 core, as index of weathering versus volcanic inputs (data from Table S2).

methane degassing provided the isotopic anomaly and ocean crisis (Kennedy *et al.*, 2008), but close examination of the locality that was the basis for that hypothesis (Retallack *et al.*, 2015) failed to find a methanogenic signature as in Figure 9. Another idea is that voluminous marine volcanism was the source of alkalisation (Gernon *et al.*, 2016). Doubt that such a catastrophic pH perturbation of the ocean was possible have come from indications that the isotopic anomalies were diagenetic (Ahm *et al.*, 2019; Kennedy, 1996; Klaebe *et al.*, 2017), perhaps by meteoric weathering as a paleokarst at a time of glacial sea-level drawdown, creating rough correlation between $\delta^{13}C$ and $\delta^{18}O$ (Figure 9d). An alternative interpretation is that the 'cap carbonates' were calcareous loess, comparable with the late Quaternary Peoria Loess of North America (Bettis *et al.*, 2003; Fisk, 1951; Grimley *et al.*, 1998; Ruhe & Olson, 1980; Swineford & Frye, 1951). Multiple lines of evidence suggest such an origin for the Nuccaleena Formation above the basal Ediacaran stratotype locality in Enorama Creek, South Australia: these include thufur mounds, climbing translatent stratification, tent structures with uniquely alternating top sets, and silt grainsize (Retallack, 2011).

Red siltstones of the Johnnys Creek Formation are dolomitic loess like the Nuccaleena Formation (Figure 6), but predates, rather than postdates, Sturtian glaciation of Areyonga Formation tillites (Figures 3 and 4). Thus, it cannot literally be a 'cap carbonate', despite chemical and petrographic similarities. Loess in deep time is commonly much redder and compacted than late Quaternary loess and requires laboratory data like Figure 6 to recognise (Pfeifer *et al.*, 2021; Retallack *et al.*, 2003; Soreghan *et al.*, 2008). If 'cap carbonates' and their isotopic crises were local loess plains rather than global oceanic pH catastrophes, are they of use for stratigraphic correlation? As in the case of the interbedded stromatolitic limestones and red loesses of the Johnnys Creek Formation, they may reflect global low sea-level at times of continental ice maxima. Johnnys Creek Formation loess is thus evidence of pre-Cryogenian glaciation, such as the 752 Ma Konnarock Formation of Virginia (McLennan et al., 2020), which is represented by a brief negative $\delta^{13}C$ anomaly in the Johnnys Creek Formation (Swanson-Hysell *et al.*, 2012). 'Cap carbonates' are a distinctive facies better regarded as calcareous loess plains formed during low sea-level, rather than an oceanic pH catastrophe (Retallack, 2011).

Glaciation induced by advances in evolution of life on land?

Evidence collected here to address the cause of Snowball Earth is assembled against the age models (Table 1) in Figure 12, in order to address the four conflicting hypotheses of (1) evolutionary advances in life on land (Retallack *et al.*, 2021); (2) evolutionary advances in marine life (Tziperman *et al.*, 2011), (3) large amounts of easily weatherable materials or aerosols produced by volcanism (Donnadieu *et al.*, 2004; Long *et al.*, 2019; MacDonald & Wordsworth, 2017; Stern & Miller, 2018), and (4) continental drift into intensely weathered, warm–humid, tropical regions of Siberian, southern African and Australian cratons (Hoffman & Li, 2009; Hoffman & Schrag, 2002). Australian paleosols described here do not show lowered molar base/alumina ratios expected for addition of fresh volcanic ash, nor large changes in atmospheric CO_2, nor paleolatitude change (Figure 12). The Johnnys Creek Formation remained at subtropical paleolatitudes (26°; Figures 3j and 12), which is commonly an arid belt of limited soil formation

(Retallack, 2019). No shards or mafic crystals from volcanic ash were seen in thin-section of the Johnnys Creek Formation and these are more likely to have been a source than a sink for greenhouse gases (Retallack & Conde, 2020).

In proposing a biotic explanation for the onset of Snowball Earth, Tziperman *et al*. (2011) invoke increased complexity and biomass of marine organisms, principally eukaryotic algae, increasing carbon burial in the ocean. The rise of algae is also considered causal by Feulner *et al*. (2015), who argued that atmospheric cooling to Snowball Earth was by algal emission of aerosolic dimethyl sulfide. This study in contrast has assembled evidence for increased biomass and effectiveness of life on land, which would in turn have fuelled marine productivity with nutrient bases. Little is known about the nature of organisms responsible for observed late Tonian increase in depth and intensity of weathering of calcareous paleosols, and transition from gypsic to calcic soil microbiomes (Figure 12). Other indirect lines of evidence for late Tonian burgeoning life on land include a variety of trends in marine rocks: decreased aluminium phosphate in nearshore marine metaquartzites (Morteani *et al*., 2007), more complex clay polytypes in marine shales (Kennedy *et al*., 2006), onset of significant paleokarst diagenesis of carbonates (Knauth & Kennedy, 2009), and higher strontium isotopic composition of marine limestones (Kennedy, 2013). Like these indirect lines of evidence, paleosols are not records as detailed as desirable, because their highly efficient mechanisms of biological recycling may preclude preservation of individual fossils (Retallack, 2012). Late Tonian organisms involved in this transformation may be represented by a variety of recently discovered megafossils (Figure 11), but their biological affinities remain controversial (Retallack, 2013a; Retallack & Broz, 2020). If the modern gypsic–calcic ecosystem transition in the Atacama Desert is a guide, then low diversity cyanobacteria-actinobacteria communities would have been enriched by fungi, archaea, algae, and protists (Araya *et al*., 2020; Castillo & Beck, 2012; Neilson *et al*., 2012, 2017; Quade *et al*., 2007; Vítek *et al*., 2013), the latter perhaps including social amoebae for trails of *Lamonte trevallis* (Retallack & Broz, 2020). A plausible biological hypothesis for Cryogenian acceleration of silicate weathering is the evolution or geographic expansion of megascopic lichens or other photosynthetic consortia on land. In other words, life on land became big and thick, much more than Paleoproterozoic life on land, known from discoidal microbial colonies and social amoebae (Retallack & Mao, 2019), small endosymbiotic fungi (Retallack, Dunn, *et al*., 2013; Retallack, Krull, *et al*., 2013), and resistant, complexly layered spore walls of fungi comparable with Glomeromycota (Loron *et al*., 2019; Retallack, 2015c). Fungal hyphae and tissue fragments are also known from Tonian, Cryogenian and Ediacaran rocks (Agić *et al*., 2019; Bonneville *et al*., 2020; Retallack *et al*., 2021). Weathering intensity under modern lichens is 2–18 times that of nearby abiotic rock surfaces (Brady *et al*., 1999). Weathering under calcic ecosystems is deeper and more intense than gypsic ecosystems and sequesters six times more soil organic carbon (Ewing *et al*., 2006, 2008).

The working hypothesis proposed here is that Snowball Earth glaciations were triggered by evolution of megascopic terrestrial organisms, perhaps eukaryotic fungi and lichens, which deepened soils, increased respired soil-CO_2, promoted chemical weathering of base cations, enlarged terrestrial biomass, and ameliorated soil salinity to create the most productive terrestrial ecosystems known up to that time. Deeper terrestrial weathering also would have delivered higher fluxes of cationic nutrients, bicarbonate, and differences in isotopic composition to marine rocks (Kennedy, 2013; Knauth & Kennedy, 2009; Morteani *et al*., 2007). Comparable biotic hypotheses for glaciation include Ordovician evolution of liverworts and mosses increasing the depth and degree of weathering on land (Lenton *et al*., 2012; Retallack, 2015b), Devonian evolution of forests with clayey (Alfisol and Ultisol) and peaty (Histosol) soils (Berner, 1997; Retallack & Huang, 2011), and Cenozoic evolution of grasslands with organic-rich (Mollisol), moist, high albedo soils (Retallack, 2013b). Compared with these other major evolutionary advances in biomass and soil carbon storage on land, fungi and lichens would have been more widespread on land because more hardy in frigid alpine and polar environments. Liverworts, trees, and grasses are more sensitive to freezing, and their latitudinal and altitudinal limits (Harsch & Bader, 2011) are lower than for cyanobacteria, algae, fungi, and lichens (Belnap *et al*., 2001). Liverworts, trees, and grasses were consecutive additions to terrestrial ecosystems (Retallack, 2013b, 2015a, 2015b: Retallack & Huang, 2011), building on, but not completely displacing a framework of lichen weathering on land that may have been established as early as the Tonian. These differences may explain why Cryogenian glaciations extended to much lower latitudes than Ordovician, Permo-Carboniferous or Pleistocene glaciations (Hoffman & Schrag, 2002; Retallack, 2011).

Acknowledgements

Adrian Broz and Will Defliese aided during fieldwork. Max Heckenberg gave access to drill cores in Alice Springs. Ilya Bindeman, Kathryn Watts, Malcolm Walter and Bruce Runnegar offered useful discussion. Christina Edgoose also helped with field directions and detailed editing of a draft of this paper.

Disclosure statement

No potential conflict of interest was reported by the author(s).

ORCID

G. J. Retallack http://orcid.org/0000-0003-4356-9240

Data availability statement

Data that support the findings of this study are available from the University of Oregon at https://blogs.uoregon.edu/gregr/detailed-web-page/downloadable-data/

References

Agić, H., Högström, A. E., Moczydłowska, M., Jensen, S., Palacios, T., Meinhold, G., Ebbestad, J. O. R., Taylor, W. L., & Høyberget, M. (2019). Organically-preserved multicellular eukaryote from the early Ediacaran Nyborg Formation, Arctic Norway. *Scientific Reports*, *9*, 1–12. https://doi.org/10.1038/s41598-019-50650-x

Ahm, A. S. C., Maloof, A. C., Macdonald, F. A., Hoffman, P. F., Bjerrum, C. J., Bold, U., Rose, C. V., Strauss, J. V., & Higgins, J. A. (2019). An early diagenetic deglacial origin for basal Ediacaran "cap dolostones. *Earth and Planetary Science Letters*, *506*, 292–307. https://doi.org/10.1016/j.epsl.2018.10.046

Aiello, I. W., Garrison, R. E., Moore, E. C., Kastner, M., & Stakes, D. S. (2001). Anatomy and origin of carbonate structures in a Miocene cold-seep field. *Geology*, *29*(12), 1111–1114. https://doi.org/10.1130/0091-7613(2001)029<1111:AAOOCS>2.0.CO;2

Al-Kofahi, M. M., Hallak, A. B., Al-Juwair, H. A., & Saafin, A. K. (1993). Analysis of desert rose using PIXE and RBS techniques. *X-Ray Spectrometry*, *22*(1), 23–27. https://doi.org/10.1002/xrs.1300220107

Álvaro, J. J., Van Vliet-Lanoë, B., Vennin, E., & Blanc-Valleron, M. M. (2003). Lower Cambrian paleosols from the Cantabrian Mountains (Northern Spain): A comparison with Neogene–Quaternary estuarine analogues. *Sedimentary Geology*, *163*(1–2), 67–84. https://doi.org/10.1016/S0037-0738(03)00159-3

Ambrose, G. J., Dunster, J. N., Munson, T. J., & Edgoose, C. J. (2010). Well completion reports for NTGS stratigraphic drillholes LA05DD01 and BR05DD01, southwestern Amadeus Basin. *Records of the Northern Territory Geological Survey*, *2010–015*, 1–30. https://geoscience.nt.gov.au/gemis/ntgsjspui/handle/1/82455

Anderson, R. P., Tarhan, L. G., Cummings, K. E., Planavsky, N. J., & Bjørnerud, M. (2016). Macroscopic structures in the 1.1 Ga continental Copper Harbor Formation: Concretions or fossils? *PALAIOS*, *31*(7), 327–338. https://doi.org/10.2110/palo.2016.013

Araya, J. P., González, M., Cardinale, M., Schnell, S., & Stoll, A. (2020). Microbiome dynamics associated with the Atacama flowering desert. *Frontiers of Microbiology*, *10*, e3160. https://doi.org/10.3389/fmicb.2019.03160

Bao, H., Chen, Z. Q., & Zhou, C. (2012). An ^{17}O record of late Neoproterozoic glaciation in the Kimberley region, Western Australia. *Precambrian Research, 216–219*(1), 151–161. https://doi.org/10.1016/j.precamres.2012.06.019

Barbour, M. M., & Farquhar, G. D. (2000). Relative humidity- and ABA-induced variation in carbon and oxygen isotope ratios of cotton leaves. *Plant Cell and Environment*, *23*(5), 473–485. https://doi.org/10.1046/j.1365-3040.2000.00575.x

Barbour, M. M., Walcroft, A. S., & Farquhar, G. D. (2002). Seasonal variation in $\delta^{13}C$ and $\delta^{18}O$ of cellulose from growth rings of *Pinus radiata*. *Plant, Cell & Environment*, *25*(11), 1483–1499. https://doi.org/10.1046/j.0016-8025.2002.00931.x

Barovich, K. M., & Foden, J. (2000). A Neoproterozoic flood basalt province in southern-central Australia: Geochemical and Nd isotope evidence from basin fill. *Precambrian Research*, *100*(1–3), 213–234. https://doi.org/10.1016/S0301-9268(99)00075-3

Belnap, J. (2003). Comparative structure of physical and biological soil crusts. In J. Belnap & O. L. Lange (Eds), *Biological soil crusts: Structure, function and management* (pp. 177–191). Springer. https://doi.org/10.1007/978-3-642-56475-8_15

Belnap, J., Kaltenecker, J. H., Rosentreter, R., Williams, J., Leonard, S., & Eldridge, D. (2001). Biological soil crusts: Ecology and management. *Bureau of Land Management Technical Reference*, *1730*, 1–110. https://www.ars.usda.gov/research/publications/publication/?seqNo115=125127

Beraldi-Campesi, H., & Retallack, G. J. (2016). Terrestrial ecosystems in the Precambrian. In B. Weber, B. Büdel, & J. Belnap (Eds), *Biological soil crusts: An organizing principle in drylands* (pp. 37–54). Springer. https://doi.org/10.1007/978-3-319-30214-0_3

Berner, R. A. (1997). The rise of plants and their effect on weathering and atmospheric CO_2. *Science*, *276*(5312), 544–546. https://doi.org/10.1126/science.276.5312.544

Bestland, E. A., Retallack, G. J., Rice, A. E., & Mindszenty, A. (1996). Late Eocene detrital laterites in central Oregon: Mass balance geochemistry, depositional setting and landscape evolution. *Geological Society of America Bulletin*, *108*(3), 285–302. https://doi.org/10.1130/0016-7606(1996)108<0285:LEDLIC>2.3.CO;2

Bettis, E. A., Mason, J. P., Swinehart, J. B., Miao, X-D., Hanson, P. R., Goble, R. J., Loope, D. B., Jacobs, P. M., & Roberts, H. M. (2003). Cenozoic eolian sedimentary systems of the USA mid-continent. In D. J. Easterbook (Ed), *Quaternary geology of the United States. INQUA 2003 field guide volume* (pp. 195–218). Desert Research Institute. https://www.worldcat.org/title/quaternary-geology-of-the-united-states-inqua-2003-field-guide-volume/oclc/1074784997

Blake, G. R., & Hartge, K. H. (1986). Bulk density. In A. Klute & A. L. Page (Eds), *Methods of soil analysis: Part 1 physical and mineralogical methods* (pp. 363–375). American Society of Agronomy.

Bobrovskiy, I., Hope, J. M., Ivantsov, A., Nettersheim, B. J., Hallmann, C., & Brocks, J. J. (2018). Ancient steroids establish the Ediacaran fossil *Dickinsonia* as one of the earliest animals. *Science*, *361*(6408), 1246–1249. https://doi.org/10.1126/science.aat7228

Bonneville, S., Delpomdor, F., Préat, A., Chevalier, C., Araki, T., Kazemian, M., Steele, A., Schreiber, A., Wirth, R., & Benning, L. G. (2020). Molecular identification of fungi microfossils in a Neoproterozoic shale rock. *Science Advances*, *6*(4), eaax7599. https://doi.org/10.1126/sciadv.aax7599

Brady, P. V., Dorn, R. I., Brazel, A. J., Clark, J., Moore, R. B., & Glidewell, T. (1999). Direct measurement of the combined effects of lichen, rainfall, and temperature on silicate weathering. *Geochimica et Cosmochimica Acta*, *63*(19–20), 3293–3300. https://doi.org/10.1016/S0016-7037(99)00251-3

Breecker, D. O., & Retallack, G. J. (2014). Refining the pedogenic carbonate atmospheric CO_2 proxy and application to Miocene CO_2. *Palaeogeography Palaeoclimatology Palaeoecology*, *406*, 1–8. https://doi.org/10.1016/j.palaeo.2014.04.012

Breyer, J. A., Busbey, A. B., Hanson, R. E., & Roy, E. C. (1995). Possible new evidence for the origin of metazoans prior to 1 Ga: Sediment-filled tubes from the Mesoproterozoic Allamoore Formation, Trans-Pecos Texas. *Geology*, *23*(3), 269–272. https://doi.org/10.1130/0091-7613(1995)023<0269:PNEFTO>2.3.CO;2

Brimhall, G. H., Chadwick, O. A., Lewis, C. J., Compston, W., Williams, I. S., Danti, K. J., Dietrich, W. E., Power, M. E., Hendricks, D., & Bratt, J. (1992). Deformational mass transport and invasive processes in soil evolution. *Science*, *255*(5045), 695–702. https://doi.org/10.1126/science.255.5045.695

Broad, N. (2008). *Eastern and central Arrernte picture dictionary* (p. 170). IAD Press. https://iadpress.com/shop/eastern-and-central-arrernte-picture-dictionary/

Brocks, J. J., Jarrett, A. J., Sirantoine, E., Hallmann, C., Hoshino, Y., & Liyanage, T. (2017). The rise of algae in Cryogenian oceans and the emergence of animals. *Nature*, *548*(7669), 578–581. https://doi.org/10.1038/nature23457

Brocks, J. J., Logan, G. A., Buick, R., & Summons, R. E. (1999). Archean molecular fossils and the early rise of eukaryotes. *Science*, *285*(5430), 1033–1036. https://doi.org/10.1126/science.285.5430.1033

Broz, A., Retallack, G. J., Maxwell, T. M., & Silva, L. C. R. (2021). A record of vapour pressure deficit preserved in wood and soil across biomes. *Scientific Reports*, *11*(1), 662. https://doi.org/10.1038/s4159 8-020-80006-9

Buggle, B., Glaser, B., Hambach, U., Gerasimenko, N., & Marković, S. (2011). An evaluation of geochemical weathering indices in

loess–paleosol studies. *Quaternary International*, *240*(1–2), 12–21. https://doi.org/10.1016/j.quaint.2010.07.019

Bureau of Meteorology. (2020). Climate statistics for Australian locations. Retrieved May 11, 2020, from http://www.bom.gov.au/climateaverages.

Butler, R. F. (1992). *Palaeomagnetism: Magnetic domains to geologic terranes*. Blackwell. https://websites.pmc.ucsc.edu/~njarboe/pmagresource/ButlerPaleomagnetismBook.pdf

Castillo, R. V., & Beck, A. (2012). Photobiont selectivity and specificity in *Caloplaca* species in a fog-induced community in the Atacama Desert, northern Chile. *Fungal Biology*, *116*(6), 665–676. https://doi.org/10.1016/j.funbio.2012.04.001

Cerling, T. E. (1991). Carbon dioxide in the atmosphere; evidence from Cenozoic and Mesozoic paleosols. *American Journal of Science*, *291*(4), 377–400. https://doi.org/10.2475/ajs.291.4.377

Chadwick, O. A., Brimhall, G. H., & Hendricks, D. M. (1990). From a black to a gray box—a mass balance interpretation of pedogenesis. *Geomorphology*, *3*(3–4), 369–390. https://doi.org/10.1016/0169-555X(90)90012-F

Chen, S., Gagnon, A. C., & Adkins, J. F. (2018). Carbonic anhydrase, coral calcification, and a new model of stable isotope vital effects. *Geochimica et Cosmochimica Acta*, *236*, 179–197. https://doi.org/10.1016/j.gca.2018.02.032

Cockbain, A. E. (1976). Modern algal stromatolites at Hamelin Pool, a hypersaline barred basin in Shark Bay, Western Australia. In M. R. Walter (Ed), *Stromatolites* (pp. 389–411). Elsevier. https://doi.org/10.1016/S0070-4571(08)71147-6

Corkeron, M. (2007). Cap carbonates' and Neoproterozoic glacigenic successions from the Kimberley region, northwest Australia. *Sedimentology*, *54*(4), 871–903. https://doi.org/10.1111/j.1365-3091.2007.00864.x

Corkeron, M. (2008). Deposition and palaeogeography of a glacigenic Neoproterozoic succession in the east Kimberley. *Sedimentary Geology*, *204*(3–4), 61–82. https://doi.org/10.1016/j.sedgeo.2007.12.010

Corkeron, M., Webb, G. E., Moulds, J., & Grey, K. (2012). Discriminating stromatolite formation modes using rare earth element geochemistry: Trapping and binding versus *in situ* precipitation of stromatolites from the Neoproterozoic Bitter Springs Formation, Northern Territory, Australia. *Precambrian Research*, *212–213*, 194–206. https://doi.org/10.1016/j.precamres.2012.04.019

Crits-Christoph, A., Robinson, C. K., Barnum, T., Fricke, W. F., Davila, A. F., Jedynak, B., McKay, C. P., & DiRuggiero, J. (2013). Colonization patterns of soil microbial communities in the Atacama Desert. *Microbiome*, *1*(1), 28–13. https://doi.org/10.1186/2049-2618-1-28

Dalrymple, R. W., Narbonne, G. M., & Smith, L. (1985). Eolian action and the distribution of Cambrian shales in North America. *Geology*, *13*(9), 607–610. https://doi.org/10.1130/0091-7613(1985)13<607:EAATDO>2.0.CO;2

Donnadieu, Y., Goddéris, Y., Ramstein, G., Nédélec, A., & Meert, J. (2004). A 'snowball Earth' climate triggered by continental break-up through changes in runoff. *Nature*, *428*(6980), 303–306. https://doi.org/10.1038/nature02408

Dornbos, S. Q., Oji, T., Kanayama, A., & Gonchigdorj, S. (2016). A new Burgess Shale-type deposit from the Ediacaran of Western Mongolia. *Scientific Reports*, *6*, 23438. https://doi.org/10.1038/srep23438

Driese, S. G., Simpson, E. L., & Eriksson, K. A. (1995). Redoximorphic paleosols in alluvial and lacustrine deposits, 1.8 Ga Lochness Formation, Mount Isa, Australia; pedogenic processes and implications for paleoclimate. *Journal of Sedimentary Research*, *65*, 675–689. https://doi.org/10.1306/D4268199-2B26-11D7-8648000102C1865D

Edgoose, C. J. (2013). Amadeus basin. In M. Ahmad & T. J. Munson (Eds), *Geology and mineral resources of the Northern Territory* (pp. 23.1–23.70). Northern Territory Geological Survey Special Publication 5. https://geoscience.nt.gov.au/gemis/ntgsjspui/handle/1/81446

Edgoose, C. J., Normington, V. J., Haines, P. W., & Allen, H. J. (2018). Revised Neoproterozoic stratigraphy in the Mount Conner area, Amadeus Basin, Northern Territory. *Northern Territory Geological Survey Record*, *2018-008*, 10 p. https://geoscience.nt.gov.au/gemis/ntgsjspui/handle/1/87576

Ehleringer, J. R., Buchmann, N., & Flanagan, L. B. (2000). Carbon isotope ratios in belowground carbon cycle processes. *Ecological Applications*, *10*(2), 412–422. 10.1890/1051-0761(2000)010 [0412:CIRIBC]2.0.CO;2

Ehleringer, J. R., & Cook, C. S. (1998). Carbon and oxygen isotope ratios of ecosystem respiration along an Oregon conifer transect: Preliminary observations based on small-flask sampling. *Tree Physiology*, *18*(8_9), 513–519. https://doi.org/10.1093/treephys/18.8-9.513

Eriksson, K. A., Simpson, E. L., Master, S., & Henry, G. (2005). Neoarchaean (c. 2.58 Ga) halite casts: Implications for palaeoceanic chemistry. *Journal of the Geological Society of London*, *162*(5), 789–799. https://doi.org/10.1144/0016-764904-120

Ewing, S. A., MacAlady, J. L., Warren-Rhodes, K., McKay, C. P., & Amundson, R. (2008). Changes in the soil C cycle at the arid-hyperarid transition in the Atacama Desert. *Journal of Geophysical Research Biogeosciences*, *113*, G02S90. https://doi.org/10.1029/2007JG000495

Ewing, S. A., Sutter, B., Owen, J., Nishiizumi, K., Sharp, W., Cliff, S. S., Perry, K., Dietrich, W., McKay, C. P., & Amundson, R. (2006). A threshold in soil formation at Earth's arid-hyperarid transition. *Geochimica et Cosmochimica Acta*, *70*(21), 5293–5322. https://doi.org/10.1016/j.gca.2006.08.020

Farquhar, G. D., & Cernusak, L. A. (2012). Ternary effects on the gas exchange of isotopologues of carbon dioxide. *Plant, Cell & Environment*, *35*(7), 1221–1231. https://doi.org/10.1111/j.1365-3040.2012.02484

Fehrenbacher, J. B., Olson, K. R., & Jansen, I. J. (1986). Loess thickness and its effect on soils in Illinois. Bulletin University of Illinois at Urbana-Champaign. College of Agriculture. Agricultural Experiment Station (USA). *Illinois Agricultural Experiment Station Bulletin*, *782*, 14 p. https://experts.illinois.edu/en/publications/loess-thickness-in-illinois

Feulner, G. (2012). The faint young Sun problem. *Review of Geophysics*, *50*, RG2006 (29 p). https://doi.org/10.1029/2011RG000375

Feulner, G., Hallmann, C., & Kienert, H. (2015). Snowball cooling after algal rise. *Nature Geoscience*, *8*(9), 659–662. https://doi.org/10.1038/ngeo2523

Fisk, H. N. (1951). Loess and Quaternary geology of the lower Mississippi Valley. *The Journal of Geology*, *59*(4), 333–356. https://doi.org/10.1086/625872

Fletcher, B. J., Beerling, D. J., Brentnall, S. J., & Royer, D. L. (2005). Fossil bryophytes as recorders of ancient CO_2 levels: Experimental evidence and a Cretaceous case study. *Global Biogeochemical Cycles*, *19*(3), GB3012. https://doi.org/10.1029/2005GB002495

Folk, R. L., & Chafetz, H. S. (2000). Bacterially induced microscale and nanoscale carbonate precipitates. In R. E. Riding & S. M. Awramik (Eds), *Microbial Sediments* (pp. 40–49). Springer. https://doi.org/10.1007/978-3-662-04036-2_6

Food & Agriculture Organization. (1978). *Soil map of the World 1: 5,000,000. Vol. X. Australasia* (p. 21). UNESCO. http://www.fao.org/3/as355e/as355e.pdf

Gallagher, T. M., & Sheldon, N. D. (2013). A new paleothermometer for forest paleosols and its implications for Cenozoic climate. *Geology*, *41*(6), 647–650. https://doi.org/10.1130/G34074.1

Gehling, J. G., & Droser, M. L. (2013). How well do fossil assemblages of the Ediacara Biota tell time? *Geology*, *41*(4), 447–450. https://doi.org/10.1130/G33881.1

Gernon, T. M., Hincks, T. K., Tyrrell, T., Rohling, E. J., & Palmer, M. R. (2016). Snowball Earth ocean chemistry driven by extensive ridge volcanism during Rodinia breakup. *Nature Geoscience*, *9*(3), 242–248. https://doi.org/10.1038/ngeo2632

Giddings, J. A., Wallace, M. W., Haines, P. W., & Mornane, K. (2010). Submarine origin for the Neoproterozoic Wonoka Canyons, South Australia. *Sedimentary Geology*, *223*(1–2), 35–50. https://doi.org/10.1016/j.sedgeo.2009.10.001

Giordani, P., Modenesi, P., & Tretiach, M. (2003). Determinant factors for the formation of the calcium oxalate minerals, weddellite and whewellite, on the surface of foliose lichens. *The Lichenologist*, *35*(3), 255–270. https://doi.org/10.1016/S0024-2829(03)00028-8

Glaessner, M. F., & Wade, M. (1966). The late Precambrian fossils from Ediacara, South Australia. *Palaeontology*, *9*, 97–103. https://www.palass.org/publications/palaeontology-journal/archive/9/4/article_pp599-628

Grazhdankin, D., & Gerdes, G. (2007). Ediacaran microbial colonies. *Lethaia*, *40*(3), 201–210. https://doi.org/10.1111/j.1502-3931.2007.00025.x

Grazhdankin, D. V., Goy, Y. Y., & Maslov, A. V. (2012). Late Riphean microbial colonies adapted to desiccating environments. *Doklady Earth Sciences*, *446*, 1157–1161. https://link.springer.com/article/10.1134/S1028334X12100157

Grey, K., Allen, H-J., Hill, A., & Haines, P. W. (2012). Neoproterozoic biostratigraphy of the Amadeus Basin. In G. J. Ambrose & J. Scott (Eds), *central Australian Basins Symposium III* (pp. 1–17). Petroleum Exploration Society of Australia. https://www.researchgate.net/profile/Peter_Haines/publication/259468587_Neoproterozoic_biostratigraphy_of_the_Amadeus_Basin/links/5464cd670cf267ed84f25c94.pdf

Grey, K., & Corkeron, M. (1998). Late Neoproterozoic stromatolites in glacigenic successions of the Kimberley region, Western Australia: Evidence for a younger Marinoan glaciation. *Precambrian Research*, *92*(1), 65–87. https://doi.org/10.1016/S0301-9268(98)00068-0

Grimley, D. A., Follmer, L. R., & McKay, E. D. (1998). Magnetic susceptibility and mineral zonation controlled by provenance in loess along the Illinois and central Mississippi Valley. *Quaternary Research*, *49*(1), 24–36. https://doi.org/10.1006/qres.1997.1947

Haile, N. S. (1975). Calculation of paleolatitudes from paleomagnetic poles. *Geology*, *3*(4), 174. https://doi.org/10.1130/0091-7613(1975)3<174:COPFPP>2.0.CO;2

Haines, P. W., & Allen, H. J. (2014). Geology of the Boord Ridges and Gordon Hills: Key stratigraphic section in the western Amadeus Basin, Western Australia. *Geological Survey of Western Australia Record*, *11*, 1–21. https://geodocs.dmirs.wa.gov.au/Web/documentlist/3/Combined/N12BP

Halverson, G. P., Wade, B. P., Hurtgen, M. T., & Barovich, K. M. (2010). Neoproterozoic chemostratigraphy. *Precambrian Research*, *182*(4), 337–350. https://doi.org/10.1016/j.precamres.2010.04.007

Harden, J. W. (1982). A quantitative index of soil development from field descriptions: Examples from a chronosequence in central California. *Geoderma*, *28*(1), 1–28. https://doi.org/10.1016/0016-7061(82)90037-4

Harsch, M. A., & Bader, M. Y. (2011). Treeline form–a potential key to understanding treeline dynamics. *Global Ecology and Biogeography*, *20*(4), 582–596. https://doi.org/10.1111/j.1466-8238.2010.00622.x

Hayes, J. L., Riebe, C. S., Holbrook, S. W., Flinchum, B. A., & Hartsough, P. C. (2019). Porosity production in weathered rock: Where volumetric strain dominates over chemical mass loss. *Science Advances*, *5*(9), eaao0834-12. https://doi.org/10.1126/sciadv.aao0834

Hill, A. C., Arouri, K., Gorjan, P., & Walter, M. R. (2000). Geochemistry of marine and nonmarine environments of a Neoproterozoic cratonic carbonate/evaporite: The Bitter Springs Formation, central Australia. In J. P. Grotzinger, & N. P. James (Eds), *Carbonate sedimentation and diagenesis in an evolving Precambrian world* (pp. 327–344). Society of Economic Paleontologists and Mineralogists Special Publication 67. http://archives.datapages.com/data/sepm_sp/SP67/Geochemistry_of_Marine_and_Nonmarine_Environments.htm

Hoffman, P. F., & Li, Z. X. (2009). A palaeogeographic context for Neoproterozoic glaciation. *Palaeogeography Palaeoclimatology Palaeoecology*, *277*(3–4), 158–172. https://doi.org/10.1016/j.palaeo.2009.03.013

Hoffman, P. F., & Schrag, D. P. (2002). The snowball Earth hypothesis: Testing the limits of global change. *Terra Nova*, *14*(3), 129–155. https://doi.org/10.1046/j.1365-3121.2002.00408.x

Hofmann, H. J., Narbonne, G. M., & Aitken, J. D. (1990). Ediacaran remains from the intertillite beds, northwestern Canada. *Geology*, *18*(12), 1199–1202. https://doi.org/10.1130/0091-7613(1990)018<1199:ERFIBI>2.3.CO;2

House, C. H., Schopf, J. W., McKeegan, K. D., Coath, C. D., Harrison, T. M., & Stetter, K. O. (2000). Carbon isotopic composition of individual Precambrian microfossils. *Geology*, *28*(8), 707–710. https://doi.org/10.1130/0091-7613(2000)28<707:CICOIP>2.0.CO;2

Huang, C-M., Wang, C-S., & Tang, Y. (2005). Stable carbon and oxygen isotopes of pedogenic carbonates in Ustic Vertisols: Implications for paleoenvironmental change. *Pedosphere*, *15*, 539–544. http://pedosphere.issas.ac.cn/trqcn/ch/reader/view_abstract.aspx?file_no=20050417&flag=1

Isbell, R. F. (1996). *The Australian soil classification, revised edition* (p. 144). CSIRO Publishing. https://www.clw.csiro.au/aclep/asc/index.htm

Kasemann, S. A., von Strandmann, P. A. P., Prave, A. R., Fallick, A. E., Elliott, T., & Hoffmann, K. H. (2014). Continental weathering following a Cryogenian glaciation: Evidence from calcium and magnesium isotopes. *Earth and Planetary Science Letters*, *396*, 66–77. https://doi.org/10.1016/j.epsl.2014.03.048

Kelka, U., Veveakis, M., Koehn, D., & Beaudoin, N. (2017). Zebra rocks: Compaction waves create ore deposits. *Scientific Reports*, *7*(1), 1–9. https://doi.org/10.1038/s41598-017-14541-3

Kennedy, M. J. (1996). Stratigraphy, sedimentology, and isotopic geochemistry of Australian Neoproterozoic postglacial cap dolostones; deglaciation, $\delta^{13}C$ excursions, and carbonate precipitation. *Journal of Sedimentary Research*, *66*(6), 1050–1064. https://doi.org/10.2110/jsr.66.1050

Kennedy, M. J. (2013). The nonlinear effects of evolutionary innovation biospheric feedbacks on qualitative environmental change: From the microbial to metazoan world. *American Naturalist*, *81*, 100–111. https://www.journals.uchicago.edu/doi/full/10.1086/670023

Kennedy, M. J., Droser, M., Mayer, L. M., Pevear, D., & Mrofka, D. (2006). Late Precambrian oxygenation; inception of the clay mineral factory. *Science*, *311*(5766), 1446–1449. https://doi.org/10.1126/science.1118929

Kennedy, M., Mrofka, D., & Von Der Borch, C. (2008). Snowball Earth termination by destabilization of equatorial permafrost methane clathrate. *Nature*, *453*(7195), 642–645. https://doi.org/10.1038/nature06961

Klaebe, R. M., Kennedy, M. J., Jarrett, A. J. M., & Brocks, J. J. (2017). Local paleoenvironmental controls on the carbon-isotope record defining the Bitter Springs Anomaly. *Geobiology*, *15*(1), 65–80. https://doi.org/10.1111/gbi.12217

Knauth, L. P., Brilli, M., & Klonowski, S. (2003). Isotope geochemistry of caliche developed on basalt. *Geochimica et Cosmochimica Acta*, *67*(2), 185–195. https://doi.org/10.1016/S0016-7037(02)01051-7

Knauth, L. P., & Kennedy, M. J. (2009). The late Precambrian greening of the Earth. *Nature*, *460*(7256), 728–732. https://doi.org/10.1038/nature08213

Knoll, A. H., & Golubic, S. (1992). Proterozoic and living cyanobacteria. In M. Schidlowski, S. Golubic, M. M. Kimberley, D. M., McKirdy, & P. A. Trudinger (Eds), *Early organic evolution: Implications for mineral and energy resources* (pp. 450–462). Springer. https://doi.org/10.1007/978-3-642-76884-2_35

Kokelj, S. V., Pisaric, M. F., & Burn, C. R. (2007). Cessation of ice-wedge development during the 20th century in spruce forests of eastern Mackenzie Delta, Northwest Territories, Canada. *Canadian Journal of Earth Sciences*, *44*(11), 1503–1515. https://doi.org/10.1139/e07-035

Komar, P. D. (1985). The hydraulic interpretation of turbidites from their grain sizes and sedimentary structures. *Sedimentology*, *32*(3), 395–407. https://doi.org/10.1111/j.1365-3091.1985.tb00519.x

Korsch, R. J., Roser, B. P., & Kamprad, J. L. (1993). Geochemical, petrographic and grain-size variations within single turbidite beds. *Sedimentary Geology*, *83*(1–2), 15–35. https://doi.org/10.1016/0037-0738(93)90180-D

Kositcin, N., Normington, V., & Edgoose, C. J. (2015). Summary of results. Joint NTGS–GA geochronology project: Amadeus Basin, July 2013–June 2014. *Northern Territory Geological Survey Record*, *2015-*

001, 1–12. https://geoscience.nt.gov.au/gemis/ntgsjspui/handle/1/82470

Lebesconte, P. (1887). Constitution générale du Massif Breton compare à celle du Finisterre. *Bulletin Societé Géologique du France*, *14*, 776–820. https://pascal-francis.inist.fr/vibad/index.php?action=getRecordDetail&idt=GEODEBRGMFR2025410

Lenton, T. M., Crouch, M., Johnson, M., Pires, N., & Dolan, L. (2012). First plants cooled the Ordovician. *Nature Geoscience*, *5*(2), 86–89. https://doi.org/10.1038/ngeo1390

Liivamägi, S., Somelar, P., Mahaney, W. C., Kirs, J., Vircava, I., & Kirsimäe, K. (2014). Late Neoproterozoic Baltic paleosol: Intense weathering at high latitude? *Geology*, *42*(4), 323–326. https://doi.org/10.1130/G35209.1

Lindsay, J. F. (1987). Upper Proterozoic evaporites in the Amadeus basin, central Australia, and their role in basin tectonics. *Geological Society of America Bulletin*, *99*(6), 852–865. https://doi.org/10.1130/0016-7606(1987)99<852:UPEITA>2.0.CO;2

Lindsay, J. F. (1989). Depositional controls on glacial facies associations in a basinal setting, Late Proterozoic, Amadeus Basin, central Australia. *Palaeogeography Palaeoclimatology Palaeoecology*, *73*(3-4), 205–232. https://doi.org/10.1016/0031-0182(89)90005-9

Lindsay, J. F. (1991). New evidence for ancient metazoan life in the late Proterozoic Heavitree Quartzite, Amadeus Basin, central Australia. In R. J. Korsch, & J. M. Kennard (Eds), *Bulletin Bureau of Mineral Resources Geology and Geophysics* (vol. *236*, pp. 91–95). Geological and Geophysical Studies in the Amadeus basin, central Australia. http://people.rses.anu.eedu.au/lambeck_k/pdf/133.pdf

Lohmann, K. G. (1988). Geochemical patterns of meteoric diagenetic systems and their application to studies of paleokarst. In N. P. James, & P. W. Choquette (Eds), *Paleokarst* (pp. 59–80). Springer. https://doi.org/10.1007/978-1-4612-3748-8_3

Long, J., Zhang, S., & Luo, K. (2019). Cryogenian magmatic activity and early life evolution. *Scientific Reports*, *9*(1), 6586. https://doi.org/10.1038/s41598-019-43177-8

Loron, C. C., François, C., Rainbird, R. H., Turner, E. C., Borensztajn, S., & Javaux, E. J. (2019). Early fungi from the Proterozoic era in Arctic Canada. *Nature*, *570*(7760), 232–235. https://doi.org/10.1038/s41586-019-1217-0

Ludvigson, G. A., González, L. A., Fowle, D. A., Roberts, J. A., Driese, S. G., Villarreal, M. A., Smith, J. J., Suarez, M. B., & Nordt, L. C. (2013). Paleoclimatic applications and modern process studies of pedogenic siderite. In S. G. Driese, & L. C. Nordt (Eds), *New frontiers in paleopedology and terrestrial paleoclimatology* (pp. 79–87). Society of Economic Paleontologists and Mineralogists Special Publication 104. https://jenrob.ku.edu/wp-content/uploads/2018/11/paleo-climate.pdf

Ludvigson, G. A., González, L. A., Metzger, R. A., Witzke, B. J., Brenner, R. L., Murillo, A. P., & White, T. S. (1998). Meteoric sphaerosiderite lines and their use for paleohydrology and paleoclimatology. *Geology*, *26*(11), 1039–1042. https://doi.org/10.1130/0091-7613(1998)026<1039:MSLATU>2.3.CO;2

MacDonald, F. A., Schmitz, M. D., Crowley, J. L., Roots, C. F., Jones, D. S., Maloof, A. C., Strauss, J. V., Cohen, P. A., Johnston, D. T., & Schrag, D. P. (2010). Calibrating the Cryogenian. *Science*, *327*(5970), 1241–1243. https://doi.org/10.1126/science.1183325

MacDonald, F. A., & Wordsworth, R. (2017). Initiation of Snowball Earth with volcanic sulfur aerosol emissions. *Geophysical Research Letters*, *44*, 1938–1946. https://doi.org/10.1002/2016GL072335

MacLennan, S. A., Eddy, M. P., Merschat, A. J., Mehra, A. K., Crockford, P. W., Maloof, A. C., Southworth, C. S., & Schoene, B. (2020). Geologic evidence for an icehouse Earth before the Sturtian global glaciation. *Science Advances*, *6*(24), eaay6647. https://doi.org/10.1126/sciadv.aay6647

McCourt, R. M., Delwiche, C. F., & Karol, K. G. (2004). Charophyte algae and land plant origins. *Trends in Ecology & Evolution*, *19*(12), 661–666.https://doi.org/10.1016/j.tree.2004.09.013

McKenzie, N., Jacquier, D., Isbell, R., & Brown, K. (2004). *Australian soils and landscapes* (p. 416). CSIRO. https://www.publish.csiro.au/book/3821/

Meert, J. G., Gibsher, A. S., Levashova, N. N., Grice, W. C., Kamenov, G. D., & Ryabinin, A. B. (2011). Glaciation and ~770 Ma Ediacara (?) fossils from the Lesser Karatau Microcontinent, Kazakhstan. *Gondwana Research*, *19*(4), 867–880. https://doi.org/10.1016/j.gr.2010.11.008

Melezhik, V. A., Fallick, A. E., Medvedev, P. V., & Makarikhin, V. V. (1999). Extreme $^{13}C_{carb}$ enrichment in ca. 2.0 Ga magnesite–stromatolite–dolomite–red beds' association in a global context: A case for the world-wide signal enhanced by a local environment. *Earth-Science Reviews*, *48*(1–2), 71–120. https://doi.org/10.1016/S0012-8252(99)00044-6

Melim, L. A., Swart, P. K., & Eberli, G. P. (2004). Mixing zone diagenesis in the subsurface of Florida and the Bahamas. *Journal of Sedimentary Research*, *74*(6), 904–913. https://doi.org/10.1306/042904740904

Meyer, M., Xiao, S., Gill, B. C., Schiffbauer, J. D., Chen, Z., Zhou, C., & Yuan, X. (2014). Interactions between Ediacaran animals and microbial mats: Insights from *Lamonte trevallis*, a new trace fossil from the Dengying Formation of South China. *Palaeogeography Palaeoclimatology Palaeoecology*, *396*, 62–74. https://doi.org/10.1016/j.palaeo.2013.12.026

Mitchell, R. L., & Sheldon, N. D. (2010). The ~1100 Ma Sturgeon Falls paleosol revisited: Implications for Mesoproterozoic weathering environments and atmospheric CO_2 levels. *Precambrian Research*, *183*(4), 738–748. https://doi.org/10.1016/j.precamres.2010.09.003

Moczydłowska, M. (2008). The Ediacaran microbiota and the survival of Snowball Earth conditions. *Precambrian Research*, *167*, 1–15. https://doi.org/10.1016/j.precamres.2008.06.008

Monger, H. C., Daugherty, L. A., Lindemann, W. C., & Liddell, C. M. (1991). Microbial precipitation of pedogenic calcite. *Geology*, *19*(10), 997–1000. https://doi.org/10.1130/0091-7613(1991)019<0997 :MPOPC>2.3.CO;2

Morteani, G., Ackermand, D., & Trappe, J. (2007). Aluminum phosphate in Proterozoic metaquartzites: Implications for the Precambrian oceanic P budget and development of life. In U. Linneman, R. D. Nance, P. Kraft, & G. Zulauf (Eds), *The evolution of the Rheic Ocean: From Avalonian–Cadomian Active Margin to Alleghenian–Variscan Collision* (pp. 579–592). Geological Society of America Special Paper 423. https://doi.org/10.1130/2007.2423(29)

Muhs, D. R., & Budahn, J. R. (2009). Geochemical evidence for African dust and volcanic ash inputs to *terra rossa* soils on carbonate reef terraces, northern Jamaica, West Indies. *Quaternary International*, *196*(1–2), 13–35. https://doi.org/10.1016/j.quaint.2007.10.026

Muhs, D. R., Bush, C. A., Stewart, K. C., Rowland, T. R., & Crittenden, R. C. (1990). Geochemical evidence of Saharan dust parent material for soils developed on Quaternary limestones of Caribbean and western Atlantic islands. *Quaternary Research*, *33*(2), 157–177. https://doi.org/10.1016/0033-5894(90)90016-E

Murphy, C. P. (1983). Point counting pores and illuvial clay in thin section. *Geoderma*, *31*(2), 133–150. https://doi.org/10.1016/0016-7061(83)90004-6

Narbonne, G. M., Laflamme, M., Greentree, C., & Trusler, P. (2009). Reconstructing a lost world: Ediacaran rangeomorphs from Spaniard's Bay, Newfoundland. *Journal of Paleontology*, *83*(4), 503–523. https://doi.org/10.1666/08-072R1.1

Navarro-González, R., Rainey, F. A., Molina, P., Bagaley, D. R., Hollen, B. J., de la Rosa, J., Small, A. M., Quinn, R. C., Grunthaner, F. J., Cáceres, L., Gomez-Silva, B., & McKay, C. P. (2003). Mars-like soils in the Atacama Desert, Chile, and the dry limit of microbial life. *Science*, *302*(5647), 1018–1021. https://doi.org/10.1126/science.1089143

Neaman, A., Chorover, J., & Brantley, S. L. (2005a). Element mobility patterns record organic ligands in soils on early Earth. *Geology*, *33*(2), 117–120. https://doi.org/10.1130/G20687.1

Neaman, A., Chorover, J., & Brantley, S. L. (2005b). Implications of the evolution of organic acid moieties for basalt weathering over geological time. *American Journal of Science*, *305*(2), 147–185. https://doi.org/10.2475/ajs.305.2.147

Neilson, J. W., Califf, K., Cardona, C., Copeland, A., Van Treuren, W., Josephson, K. L., Knight, R., Gilbert, J. A., Quade, J., Caporaso, J. G., & Maier, R. M. (2017). Significant impacts of increasing aridity on the arid soil microbiome. *mSystems*, *2*(3), e00195–16. https://doi.org/10.1128/mSystems.00195-16

Neilson, J. W., Quade, J., Ortiz, M., Nelson, W. M., Legatzki, A., Tian, F., LaComb, M., Betancourt, J. L., Wing, R. A., Soderlund, C. A., & Maier, R. M. (2012). Life at the hyperarid margin: Novel bacterial diversity in arid soils of the Atacama Desert, Chile. *Extremophiles*, *16*(3), 553–566. https://doi.org/10.1007/s00792-012-0454-z

Neraudeau, D., Dabard, M-P., El Albani, A., Gougeon, R., Mazurier, A., Pierson-Wickmann, A-C., Poujol, M., Saint Martin, J-P., & Saint Martin, S. (2018). First evidence of Ediacaran–Fortunian elliptical body fossils in the Brioverian series of Brittany, NW France. *Lethaia*, *51*(4), 513–522. https://doi.org/10.1111/let.12270

Noffke, N. (2010). *Geobiology: Microbial mats in sandy deposits from the Archean Era to today* Springer. https://www.springer.com/gp/book/9783642127717

Normington, V. J., Beyer, E. E., Whelan, J. A., Edgoose, C. J., & Woodhead, J. D. (2019). Summary of results. NTGS LA-ICP-MS Hf program: Amadeus Basin, July 2013–June 2015. *Northern Territory Geological Survey Record, 2019-005*, p. 34 https://geoscience.nt.gov.au/gemis/ntgsjspui/handle/1/88593

Normington, V. J., Edgoose, C. J., Donnellan, N., Weisheit, A., & Verdel, C. (2019). New insights into the Neoproterozoic to early Palaeozoic stratigraphy, structure and palaeogeography of the Amadeus Basin, Northern Territory. *Northern Territory Geological Survey Record, 2019-003*, 129−133. https://geoscience.nt.gov.au/gemis/ntgsjspui/handle/1/88365

Novoselov, A. A., & de Souza Filho, C. R. (2015). Potassium metasomatism of Precambrian paleosols. *Precambrian Research*, *262*, 67–83. https://doi.org/10.1016/j.precamres.2015.02.024

Oehler, D. Z. (1976). Transmission electron microscopy of organic microfossils from the late Precambrian Bitter Springs Formation of Australia: Techniques and survey of preserved ultrastructure. *Journal of Paleontology*, *50*, 90–106. https://www.jstor.org/stable/1303642

Oehler, D. Z. (1977). Pyrenoid-like structures in late Precambrian algae from the Bitter Springs Formation of Australia. *Journal of Paleontology*, *51*, 885–901. https://www.jstor.org/stable/1303761

Óskarsson, B. V., Riishuus, M. S., & Arnalds, Ó. (2012). Climate-dependent chemical weathering of volcanic soils in Iceland. *Geoderma*, *189-190*, 635–651. https://doi.org/10.1016/j.geoderma.2012.05.030

Peckmann, J., Goedert, J. L., Thiel, V., Michaelis, W., & Reitner, J. (2002). A comprehensive approach to the study of methane-seep deposits from the Lincoln Creek Formation, western Washington State, USA. *Sedimentology*, *49*(4), 855–873. https://doi.org/10.1046/j.1365-3091.2002.00474.x

Pfeifer, L. S., Soreghan, G. S., Pochat, S., & Van Den Driessche, J. (2021). Loess in eastern equatorial Pangea archives a dusty atmosphere and possible upland glaciation. *GSA Bulletin*, *133*(1–2), 379–392. https://doi.org/10.1130/B35590.1

Porter, S. M., & Knoll, A. H. (2000). Testate amoebae in the Neoproterozoic Era: Evidence from vase-shaped microfossils in the Chuar Group, Grand Canyon. *Paleobiology*, *26*(3), 360–385. https://doi.org/10.1666/0094-8373(2000)026<0360:TAITNE>2.0.CO;2

Porter, S. M., Meisterfeld, R., & Knoll, A. H. (2003). Vase-shaped microfossils from the Neoproterozoic Chuar Group, Grand Canyon: a classification guided by modern testate amoebae. *Journal of Paleontology*, *77*(3), 409–429. https://doi.org/10.1666/0022-3360(2003)077<0409:VMFTNC>2.0.CO;2

Prave, A. R. (2002). Life on land in the Proterozoic: Evidence from the Torridonian rocks of northwest Scotland. *Geology*, *30*(9), 811. https://doi.org/10.1130/0091-7613(2002)030<0811:LOLITP>2.0.CO;2

Prins, M. A., Vriend, M., Nugteren, G., Vandenberghe, J., Lu, H., Zheng, H., & Weltje, G. J. (2007). Late Quaternary aeolian dust input variability on the Chinese Loess Plateau: Inferences from unmixing of loess grain-size records. *Quaternary Science Reviews*, *26*(1–2), 230–242. https://doi.org/10.1016/j.quascirev.2006.07.002

Pye, K., & Sherwin, D. (1999). Loess. In A. S. Goudie, I. Livingstone, & S. Stokes (Eds), *Aeolian environments, sediments and landforms* (pp. 213–238). Wiley.

Quade, J., Rech, J. A., Latorre, C., Betancourt, J. L., Gleeson, E., & Kalin, M. T. (2007). Soils at the hyperarid margin: The isotopic composition of soil carbonate from the Atacama Desert, Northern Chile. *Geochimica et Cosmochimica Acta*, *71*(15), 3772–3795. https://doi.org/10.1016/j.gca.2007.02.016

Raffi, R., & Stenni, B. (2011). Isotopic composition and thermal regime of ice wedges in Northern Victoria Land, East Antarctica. *Permafrost and Periglacial Processes*, *22*(1), 65–83. https://doi.org/10.1002/ppp.701

Rech, J. A., Quade, J., & Hart, W. S. (2003). Isotopic evidence for the source of Ca and S in soil gypsum, anhydrite and calcite in the Atacama Desert, Chile. *Geochimica et Cosmochimica Acta*, *67*(4), 575–586. https://doi.org/10.1016/S0016-7037(02)01175-4

Renaut, R. W., & Tiecerlin, J-J. (1994). Lake Bogoria, Kenya Rift Valley − A sedimentological overview. In R. W. Renaut, & W. M. Last (Eds), *Sedimentology and geochemistry of modern and ancient saline lakes* (pp. 101–124). Society for Sedimentary Geology Special Publication 50. http://archives.datapages.com/data/sepm_sp/SP50/Lake_Bogoria.htm

Retallack, G. J. (1976). Triassic palaeosols in the upper Narrabeen Group of New South Wales. Part I: Features of the palaeosols. *Journal of the Geological Society of Australia*, *23*(4), 383–399. https://doi.org/10.1080/00167617608728953

Retallack, G. J. (1991a). Untangling the effects of burial alteration and ancient soil formation. *Annual Review of Earth and Planetary Sciences*, *19*(1), 183–206. https://doi.org/10.1146/annurev.ea.19.050191.001151

Retallack, G. J. (1991b). *Miocene paleosols and ape habitats of Pakistan and Kenya*. Oxford University Press.

Retallack, G. J. (1992). What to call early plant formations on land. *Palaios*, *7*(5), 508–520. https://doi.org/10.2307/3514848

Retallack, G. J. (2005). Pedogenic carbonate proxies for amount and seasonality of precipitation in paleosols. *Geology*, *33*(4), 333–336. https://doi.org/10.1130/G21263.1

Retallack, G. J. (2008). Cambrian paleosols and landscapes of South Australia. *Australian Journal of Earth Sciences*, *55*(8), 1083–1106. https://doi.org/10.1080/08120090802266568

Retallack, G. J. (2011). Neoproterozoic loess and limits to Snowball Earth. *Journal of the Geological Society of London*, *168*(2), 289–308. https://doi.org/10.1144/0016-76492010-051

Retallack, G. J. (2012). Criteria for distinguishing microbial mats and earths. In N. Noffke & H. Chafetz (Eds), *Microbial mats in siliciclastic sediments* (pp. 136–152). Society of Economic Paleontologists and Mineralogists Special Paper 101. https://doi.org/10.2110/sepmsp.101.139

Retallack, G. J. (2013a). Ediacaran life on land. *Nature*, *493*(7430), 89–92. https://doi.org/10.1038/nature11777

Retallack, G. J. (2013b). Global cooling by grasslands in the geological past and near future. *Annual Review of Earth and Planetary Sciences*, *41*(1), 69–86. https://doi.org/10.1146/annurev-earth-050212-124001

Retallack, G. J. (2015a). Silurian vegetation stature and density inferred from fossil soils and plants in Pennsylvania, U.S.A. *Journal of the Geological Society of London*, *172*(6), 693–709. https://doi.org/10.1144/jgs2015-022

Retallack, G. J. (2015b). Late Ordovician glaciation initiated by early land plant evolution, and punctuated by greenhouse mass-extinctions. *The Journal of Geology*, *123*(6), 509–538. https://doi.org/10.1086/683663

Retallack, G. J. (2015c). Acritarch evidence for an Ediacaran adaptive radiation of Fungi. *Botanica Pacifica*, *4*, 19–33. https://doi.org/10.17581/bp.2015.04203

Retallack, G. J. (2016). Field and laboratory tests for recognition of Ediacaran paleosols. *Gondwana Research*, *36*, 107–110. https://doi.org/10.1016/j.gr.2016.05.001

Retallack, G. J. (2019). *Soils of the past*. Wiley. https://doi.org/10.1002/9780470698716

Retallack, G. J., & Broz, A. P. (2020). *Arumberia* and other Ediacaran–Cambrian fossils of central Australia. *Historical Biology*, *32*, 1755281. https://doi.org/10.1080/08912963.2020.175581

Retallack, G. J., Broz, A. P., Lai, L. S. H., & Gardner, K. (2021). Neoproterozoic marine chemostratigraphy, or eustatic sea level change? *Palaeogeography, Palaeoclimatology, Palaeoecology*, *562*, 110155. https://doi.org/10.1016/j.palaeo.2020.110155

Retallack, G. J., & Conde, G. D. (2020). Deep time perspective on rising atmospheric CO_2. *Global and Planetary Change*, *189*, 103177. https://doi.org/10.1016/j.gloplacha.2020.103177

Retallack, G. J., Dunn, K. L., & Saxby, J. (2013). Problematic Mesoproterozoic fossil *Horodyskia* from Glacier National Park, Montana, USA. *Precambrian Research*, *226*, 125–142. https://doi.org/10.1016/j.precamres.2012.12.005

Retallack, G. J., Gose, B. N., & Osterhout, J. T. (2015). Periglacial paleosols and Cryogenian paleoclimate near Adelaide, South Australia. *Precambrian Research*, *263*, 1–18. https://doi.org/10.1016/j.precamres.2015.03.002

Retallack, G. J., & Huang, C-M. (2010). Depth to gypsic horizon as a proxy for paleoprecipitation in paleosols of sedimentary environments. *Geology*, *38*(5), 403–406. https://doi.org/10.1130/G30514.1

Retallack, G. J., & Huang, C-M. (2011). Ecology and evolution of Devonian trees in New York, USA. *Palaeogeography Paleoclimatology Paleoecology*, *299*(1–2), 110–128. https://doi.org/10.1016/j.palaeo.2010.10.040

Retallack, G. J., & Jahren, A. H. (2008). Methane release from igneous intrusion of coal during Late Permian extinction events. *The Journal of Geology*, *116*(1), 1–20. https://doi.org/10.1086/524120

Retallack, G. J., Krull, E. S., Thackray, G. D., & Parkinson, D. (2013). Problematic urn-shaped fossils from a Paleoproterozoic (2.2 Ga) paleosol in South Africa. *Precambrian Research*, *235*, 71–87. https://doi.org/10.1016/j.precamres.2013.05.015

Retallack, G. J., & Mao, X. (2019). Paleoproterozoic (ca. 1.9 Ga) megascopic life on land in Western Australia. *Palaeogeography Palaeoclimatology Palaeoecology*, *532*, 109266. https://doi.org/10.1016/j.palaeo.2019.109266

Retallack, G. J., Marconato, A., Osterhout, J. T., Watts, K. E., & Bindeman, I. N. (2014). Revised Wonoka isotopic anomaly in South Australia and Late Ediacaran mass extinction. *Journal of the Geological Society of London*, *171*(5), 709–722. https://doi.org/10.1144/jgs2014-016

Retallack, G. J., & Mindszenty, A. (1994). Well preserved Late Precambrian paleosols from northwest Scotland. *Journal of Sedimentary Research*, A64, 264−281. https://doi.org/10.1306/D4267D7A-2B26-11D7-8648000102C1865D

Retallack, G. J., Smith, R. M., & Ward, P. D. (2003). Vertebrate extinction across Permian–Triassic boundary in Karoo Basin, South Africa. *Geological Society of America Bulletin*, *115*(9), 1133–1152. https://doi.org/10.1130/B25215.1

Romanek, C. S., Grossman, E. L., & Morse, J. W. (1992). Carbon isotopic fractionation in synthetic aragonite and calcite: Effects of temperature and precipitation rate. *Geochimica et Cosmochimica Acta*, *56*(1), 419–430. https://doi.org/10.1016/0016-7037(92)90142-6

Rosentreter, R. (1984). Compositional patterns within a rabbitbrush (*Chrysothamnus*) community of the Idaho Snake River Plain. *Intermountain Research Station General Technical Report*, INT-200, 273–277.

Ruhe, R. V., & Olson, C. G. (1980). Clay mineral indicators of glacial and non-glacial sources of Wisconsinan loesses in southern Indiana, USA. *Geoderma*, *24*(4), 283–297. https://doi.org/10.1016/0016-7061(80)90056-7

Schmid, S. (2017). Neoproterozoic evaporites and their role in carbon isotope chemostratigraphy (Amadeus Basin, Australia). *Precambrian Research*, *290*, 16–31. https://doi.org/10.1016/j.precamres.2016.12.004

Schopf, J. W. (1968). Microflora of the Bitter Springs formation, late Precambrian, central Australia. *Journal of Paleontology*, *42*, 651–688. https://www.jstor.org/stable/1302368

Schopf, J. W., & Blacic, J. M. (1971). New microorganisms from the Bitter Springs Formation (late Precambrian) of the north-central Amadeus Basin, Australia. *Journal of Paleontology*, *45*, 925–960. https://www.jstor.org/stable/1302822

Scotese, C. R. (2009). Late Proterozoic plate tectonics and palaeogeography: A tale of two supercontinents, Rodinia and Pannotia. In J. Craig, J. Thurow, B. Thusu, A Whitham, & Y. Abutarruma (Eds), *Global Neoproterozoic petroleum systems: The emerging potential in North Africa* (pp. 67–83). Geological Society of London Special Publication, 326. https://doi.org/10.1144/SP326.4

Serezhnikova, E. A., Ragozina, A. L., Dorjnamjaa, D., & Zaitseva, L. V. (2014). Fossil microbial communities in Neoproterozoic interglacial rocks, Maikhanuul formation, Zavkhan basin, Western Mongolia. *Precambrian Research*, *245*, 66–79. https://doi.org/10.1016/j.precamres.2014.01.005

Sheldon, N. D. (2006). Precambrian paleosols and atmospheric CO_2 levels. *Precambrian Research*, *147*(1–2), 148–155. https://doi.org/10.1016/j.precamres.2006.02.004

Sheldon, N. D., & Retallack, G. J. (2001). Equation for compaction of paleosols due to burial. *Geology*, *29*(3), 247–250. https://doi.org/10.1130/0091-7613(2001)029<0247:EFCOPD>2.0.CO;2

Sheldon, N. D., Retallack, G. J., & Tanaka, S. (2002). Geochemical climofunctions from North American soils and application to paleosols across the Eocene–Oligocene boundary in Oregon. *The Journal of Geology*, *110*(6), 687–696. https://doi.org/10.1086/342865

Sheldon, N. D., & Tabor, N. J. (2013). Using paleosols to understand paleo-carbon burial. In S. G. Dreise, & L. Nordt (Eds), *New frontiers in paleopedology and terrestrial paleoclimatology: Paleosols and soil surface analog systems* (pp. 71–78). Society of Economic Paleontologists and Mineralogists Special Publication 104. https://doi.org/10.2110/sepmsp.104.11

Skotnicki, S. J., Hill, A. C., Walter, M., & Jenkins, R. (2008). Stratigraphic relationships of Cryogenian strata disconformably overlying the Bitter Springs Formation, northeastern Amadeus Basin, central Australia. *Precambrian Research*, *165*(3–4), 243–259. https://doi.org/10.1016/j.precamres.2008.06.013

Smith, B. R. (2011). Drillhole report for BR05DD01, Amadeus Basin, Northern Territory: National Virtual Core Library NTGS Node: HyLogger 2–7. *Northern Territory Geological Survey Record*, *2011-002*, 1–18. https://geoscience.nt.gov.au/gemis/ntgsjspui/handle/1/82004

Soil Survey Staff. (2014). *Keys to soil taxonomy* (p. 358). Natural Resources Conservation Service. https://www.nrcs.usda.gov/wps/portal/nrcs/detail/soils/survey/class/taxonomy/?cid=nrcs142p2_053580

Soreghan, G. S., Soreghan, M. J., & Hamilton, M. A. (2008). Origin and significance of loess in late Paleozoic western Pangaea: A record of tropical cold? *Palaeogeography Palaeoclimatology Palaeoecology*, *268*(3–4), 234–259. https://doi.org/10.1016/j.palaeo.2008.03.050

Southgate, P. N. (1986). Depositional environment and mechanism of preservation of microfossils, upper Proterozoic Bitter Springs Formation, Australia. *Geology*, *14*(8), 683–686. https://doi.org/10.1130/0091-7613(1986)14<683:DEAMOP>2.0.CO;2

Southgate, P. N. (1989). Relationships between cyclicity and stromatolite form in the Late Proterozoic Bitter Springs Formation. *Sedimentology*, *36*(2), 323–339. https://doi.org/10.1111/j.1365-3091.1989.tb00610.x

Southgate, P. N. (1991). A sedimentological model for the Loves Creek Member of the Bitter Springs Formation, northern Amadeus Basin. In R. J. Korsch, & J. M. Kennard (Eds), *Geological and geophysical studies in the Amadeus Basin, central Australia* (pp. 113–126). Bulletin of the Bureau of Mineral Resources Geology and

Geophysics, Canberra, 236. https://ui.adsabs.harvard.edu/abs/1991ggsa.rept.113S/abstract

Stace, H. C. T., Hubble, G. D., Brewer, R., Northcote, K. H., Sleeman, J. R., Mulcahy, M. J., & Hallsworth, E. G. (1968). *A handbook of Australian soils*. Rellim. https://catalogue.nla.gov.au/Record/2546216

Stern, R. J., & Miller, N. R. (2018). Did the transition to plate tectonics cause Neoproterozoic Snowball Earth? *Terra Nova*, *30*(2), 87–94. https://doi.org/10.1111/ter.12321

Stimson, M. R., Miller, R. F., MacRae, R. A., & Hinds, S. J. (2017). An ichnotaxonomic approach to wrinkled microbially induced sedimentary structures. *Ichnos*, *24*(4), 291–316. https://doi.org/10.1080/10420940.2017.1294590

Strother, P. K., Taylor, W. A., Beck, J. H., & Vecoli, M. (2017). Ordovician spore 'thalli' and the evolution of the plant sporophyte. *Palynology*, *41*(sup1), 57–68. https://doi.org/10.1080/01916122.2017.1361213

Summons, R. E., & Walter, M. R. (1990). Molecular fossils and microfossils of prokaryotes and protists from Proterozoic sediments. *American Journal of Science*, *290*(A), 212–244. http://earth.geology.yale.edu/ajs/1990/11.1990.09SpecialSummons.pdf

Surge, D. M., Savarese, M., Dodd, J. R., & Lohmann, K. C. (1997). Carbon isotopic evidence for photosynthesis in Early Cambrian oceans. *Geology*, *25*(6), 503–506. https://doi.org/10.1130/0091-7613(1997)025<0503:CIEFPI>2.3.CO;2

Swanson-Hysell, N. L., Maloof, A. C., Kirschvink, J. L., Evans, D. A., Halverson, G. P., & Hurtgen, M. T. (2012). Constraints on Neoproterozoic paleogeography and Paleozoic orogenesis from paleomagnetic records of the Bitter Springs Formation, Amadeus Basin, central Australia. *American Journal of Science*, *312*(8), 817–884. https://doi.org/10.2475/08.2012.01

Swanson-Hysell, N. L., Rose, C. V., Calmet, C. C., Halverson, G. P., Hurtgen, M. T., & Maloof, A. C. (2010). Cryogenian glaciation and the onset of carbon-isotope decoupling. *Science*, *328*(5978), 608–611. https://doi.org/10.1126/science.1184508

Swineford, A., & Frye, J. C. (1951). Petrography of the Peoria loess in Kansas. *The Journal of Geology*, *59*(4), 306–322. https://doi.org/10.1086/625870

Talbot, M. R. (1990). A review of the palaeohydrological interpretation of carbon and oxygen isotopic ratios in primary lacustrine carbonates. *Chemical Geology: Isotope Geoscience Section*, *80*(4), 261–279. https://doi.org/10.1016/0168-9622(90)90009-2

Taylor, R. S., Hawco, J. B., Nichols, R., & McIlroy, D. (2019). A critical reappraisal of the holotype of *Beothukis mistakensis*, a unique exceptionally preserved rangeomorph organism from Mistaken Point, Newfoundland, Canada. *Estudios Geológicos*, *75*(2), e117. https://doi.org/10.3989/egeol.43586.572

Terry, R. D., & Chilingar, G. V. (1955). Summary of "Concerning some additional aids in studying sedimentary formations," by MS Shvetsov. *Journal of Sedimentary Research*, *25*(3), 229–234. https://doi.org/10.1306/74D70466-2B21-11D7-8648000102C1865D

Tziperman, E., Halevy, I., Johnston, D. T., Knoll, A. H., & Schrag, D. P. (2011). Biologically induced initiation of Neoproterozoic snowball-Earth events. *Proceedings of the National Academy of Sciences of the United States of America*, *108*(37), 15091–15096. https://doi.org/10.1073/pnas.1016361108

Ufnar, D. F., Gröcke, D. R., & Beddows, P. A. (2008). Assessing pedogenic calcite stable isotope values; can positive linear covariant trends be used to quantify palaeo-evaporation rates? *Chemical Geology*, *256*(1–2), 46–51. https://doi.org/10.1016/j.chemgeo.2008.07.022

Veizer, J., Ala, D., Azmy, K., Bruckschen, P., Buhl, D., Bruhn, F., Carden, G. A. F., Diener, A., Ebneth, S., Godderis, Y., Jasper, T., Korte, C., Pawellek, F., Podlaha, O. G., & Strauss, H. (1999). $^{87}Sr/^{86}Sr$, $\delta^{13}C$ and $\delta^{18}O$ evolution of Phanerozoic seawater. *Chemical Geology*, *161*(1–3), 59–88. https://doi.org/10.1016/S0009-2541(99)00081-9

Verrecchia, E. P., Dumont, J-L., & Verrecchia, K. E. (1993). Role of calcium oxalate biomineralization by fungi in the formation of calcretes: A case study from Nazareth. *Israel. Journal of Sedimentary Petrology*, *63*, 1000–1006. https://doi.org/10.1306/D4267C6C-2B26-11D7-8648000102C1865D

Vítek, P., Cámara-Gallego, B., Edwards, H. G., Jehlička, J., Ascaso, C., & Wierzchos, J. (2013). Phototrophic community in gypsum crust from the Atacama Desert studied by Raman spectroscopy and microscopic imaging. *Geomicrobiology Journal*, *30*(5), 399–410. https://doi.org/10.1080/01490451.2012.697976

Wallace, M. W., & Hood, A. S. (2018). Zebra textures in carbonate rocks: Fractures produced by the force of crystallization during mineral replacement. *Sedimentary Geology*, *368*, 58–67. https://doi.org/10.1016/j.sedgeo.2018.03.009

Walter, M. R. (1976). *Stromatolites*. Elsevier.

Walter, M. R., Krylov, I. N., & Preiss, W. V. (1979). Stromatolites from Adelaidean (late Proterozoic) sequences in central and South Australia. *Alcheringa: An Australasian Journal of Palaeontology*, *3*(4), 287–305. https://doi.org/10.1080/03115517908527799

Walter, M. R., Veevers, J. J., Calver, C. R., & Grey, K. (1995). Neoproterozoic stratigraphy of the Centralian Superbasin. *Precambrian Research*, *73*(1–4), 173–195. https://doi.org/10.1016/0301-9268(94)00077-5

Walter, M. R. (1972). Stromatolites and the biostratigraphy of the Australian Precambrian and Cambrian. *Special Papers in Palaeontology*, *11*, 1–190. http://go.palass.org/3c3

Watson, A. (1985). Structure, chemistry and origins of gypsum crusts in southern Tunisia and the central Namib Desert. *Sedimentology*, *32*(6), 855–875. https://doi.org/10.1111/j.1365-3091.1985.tb00737.x

Weinberger, R. (2001). Evolution of polygonal patterns in stratified mud during desiccation: The role of flaw distribution and layer boundaries. *Geological Society of America Bulletin*, *113*(1), 20–31. https://doi.org/10.1130/0016-7606(2001)113<0020:EOPPIS>2.0.CO;2

Wells, A. T., Ranford, L. C., Stewart, A. J., Cook, P. J., & Shaw, R. D. (1967). Geology of the north-eastern part of the Amadeus Basin. Northern Territory. *Bureau of Mineral Resources Geology and Geophysics Report*, *113*, 1–93. https://data.gov.au/dataset/ds-ga-a05f7892-9a60-7506-e044-00144fdd4fa6/details?q=

Werner, M., Dutch, R., Pawley, M., & Krapf, C. (2018). Amata Dolerite, Musgrave Province: Connections to Neoproterozoic mantle plume magmatism within Rodinia. *Mineral Exploration Society of Australia Journal*, *87*, 34–45. https://energymining.sa.gov.au/petroleum/data_and_publications/mesa_journal/previous_feature_articles/amata_dolerite

Yu, W., Algeo, T. J., Zhou, Q., Du, Y., & Wang, P. (2020). Cryogenian cap carbonate models: A review and critical assessment. *Palaeogeography Palaeoclimatology Palaeoecology*, *552*, 109727. https://doi.org/10.1016/j.palaeo.2020/109727

Zakrzewska, B. (1963). An analysis of landforms in a part of the central Great Plains. *Annals of the Association of American Geographers*, *53*(4), 536–568. https://doi.org/10.1111/j.1467-8306.1963.tb00465.x

Zang, W., & Walter, M. R. (1992). Late Proterozoic and Cambrian microfossils and biostratigraphy, Amadeus Basin, central Australia. *Memoirs of the Association of Australasian Palaeontolologists*, *12*, 1–132. https://catalogue.nla.gov.au/Record/2640169

Zhao, J. X., McCulloch, M. T., & Korsch, R. J. (1994). Characterization of a plume-related ~800 Ma magmatic event and its implications for basin formation in central southern Australia. *Earth and Planetary Science Letters*, *121*, 349–367. https://doi.org/10.1016/0012-821X(94)90077-9

Zhao, J. X., & Bennett, V. C. (1995). SHRIMP U/ Pb zircon geochronology of granites in the Arunta Inlier, central Australia: Implications for Proterozoic crustal evolution. *Precambrian Research*, *71*(1–4), 17–43. https://doi.org/10.1016/0301-9268(94)00054-U

Ziegenbalg, S. B., Brunner, B., Rouchy, J. M., Birgel, D., Pierre, C., Böttcher, M. E., Caruso, A., Immenhauser, A., & Peckmann, J. (2010). Formation of secondary carbonates and native sulphur in sulphate-rich Messinian strata. *Sedimentary Geology*, *227*(1–4), 37–50. https://doi.org/10.1016/j.sedgeo.2010.03.007

Zillen, L. M., Snowball, I. F., Sandgren, P., & Stanton, T. (2008). Occurrence of varved lake sediment sequences in Vamtland, west central Sweden: Lake characteristics, varve chronology and AMS radiocarbon dating. *Boreas*, *32*(4), 612–626. https://doi.org/10.1111/j.1502-3885.2003.tb01239.x